Supporting Information for:

Environmental Life Cycle Comparison of Algae to Other Bioenergy Feedstocks

Andres F. Clarens, Eleazer P. Resurreccion, Mark A. White, and Lisa M. Colosi

**1 MODEL OVERVIEW ..... 2**
1.1 FUNCTIONAL UNIT: ..... 2
1.2 SOLAR RADIATION AND METEOROLOGICAL DATA: ..... 2
*1.2.1 Insolation.* ..... *2*
*1.2.2 Miscellaneous Meteorological Parameters* ..... *2*
*1.2.3 Precipitation* ..... *3*
*1.2.4 Evaporation* ..... *3*
*1.2.5 Evapotranspiration* ..... *4*
*1.2.6 Summary* ..... *4*
1.3 CROP YIELD ESTIMATES ..... 6
*1.3.1 Corn* ..... *6*
*1.3.2 Switchgrass* ..... *7*
*1.3.3 Canola* ..... *8*
*1.3.4 Algae* ..... *10*
1.4 SELECTION OF OPEN PONDS V. PHOTOBIOREACTORS ..... 13
1.5 ALGAE STOICHIOMETRY AND FERTILIZER REQUIREMENTS ..... 13
*1.5.1 Algae Stoichiometry* ..... *13*
*1.5.2 Fertilizer Requirements* ..... *14*
1.6 HIGH HEATING VALUES OF BIOMASS STOCKS ..... 14
1.7 CORN VERSUS CORN KERNEL AND CANOLA VERSUS CANOLA SEED ..... 16

**2 IMPACT FACTOR DEFINITIONS ..... 16**
2.1 LAND USE ..... 16
2.2 WATER USE ..... 16
2.3 ENERGY USE ..... 16
2.4 GLOBAL WARMING POTENTIAL ..... 16
2.5 EUTROPHICATION ..... 17

**3 IMPACT FACTOR CALCULATIONS ..... 17**
3.1 LAND USE ..... 17
3.2 WATER USE ..... 17
3.3 ENERGY USE ..... 18
*3.3.1 Mixing* ..... *18*
*3.3.2 Centrifugation* ..... *19*
*3.3.3 Water supply* ..... *19*
*3.3.4 Infrastructure Manufacturing* ..... *20*
*3.3.5 Other* ..... *20*
3.4 GLOBAL WARMING POTENTIAL ..... 20
3.5 EUTROPHICATION ..... 20

**4 LIFE CYCLE INVENTORY DATA ..... 21**
4.1 CANOLA, CORN, AND SWITCHGRASS PRODUCTION ..... 21
4.2 ALGAE PRODUCTION ..... 21

**5 SYNERGIES WITH MUNICIPAL WASTEWATER TREATMENT ..... 21**
5.1 WASTEWATER EFFLUENTS ..... 21
5.2 MODELING BURDEN OFFSETS ..... 22
*5.2.1 Offset Fertilizer Production Burdens ..... 22*
*5.2.2 Offset Wastewater Treatment Burdens ..... 22*
*5.2.3 Offset Freshwater Burdens ..... 23*
5.3 WASTEWATER TREATMENT LIFE CYCLE INVENTORY DATA ..... 23
**6 ADDITIONAL RESULTS ..... 24**
6.1 TORNADO PLOTS ..... 24
6.2 RESULTS DISTRIBUTIONS ..... 25

# 1 Model overview

## 1.1 Functional Unit:

The functional unit (FU) selected for this study is 3 x $10^8$ BTU (317 GJ). This is the approximate per capita consumption of total primary energy for one American in one year [1]. This value reflects all energy consumed including upstream impacts associated with power production. The results are expressed using an energy functional unit to provide a reasonable comparison between dissimilar biomass feedstocks. It also provides a reasonably intuitive amount of energy that can be used to foster discussion around the "footprint" of energy consumption. The FU was also selected under the assumption that the biomass could be directly burned to produce bioelectricity and not further processed to produce a refined liquid fuel product. This avoids the inefficiency and uncertainty associated with downstream processes of the biomass into liquid fuels, which was outside the scope of this study.

## 1.2 Solar Radiation and Meteorological Data:

### *1.2.1 Insolation.*

Thirty years of insolation and selected meteorological data (1961-1990) were downloaded from the National Solar Radiation Database (NSRDB) maintained by the National Renewable Energy Laboratory (NREL) [2]. Monthly averages of daily total solar radiation over the global horizontal element (G) were obtained from observation stations in Mason City, Iowa (IA); Roanoke, Virginia (VA); and San Diego, California (CA). All of these locations are in the United States.

The fraction of total solar energy available for plants to use in photosynthesis is referred to as photosynthetically active radiation (PAR) and spans the range of wavelengths between 400 and 700 nm. PAR measurements were computed by multiplying total radiation (G) at each location by 0.46, a fraction appropriate for the range of latitudes investigated in this study [3, 4]. Histograms of monthly PAR at each location were constructed in Minitab®. The normal distribution was found to be the best fit for each monthly PAR dataset on the basis of Anderson-Darling statistics computed by the statistical software.

### *1.2.2 Miscellaneous Meteorological Parameters*

Additional meteorological measurements taken from the 1961-1990 NSRDB datasets for the selected locations include: average daily temperature, average relative humidity, and average wind speed. Histograms of monthly values for these parameters were constructed in Minitab®. The normal distribution was found to be the best fit for each dataset on the basis of Anderson-Darling statistics.

*1.2.3 Precipitation*

Thirty years of precipitation data (1979-2008) were downloaded from the National Climatic Data Center (NCDC) maintained by the National Oceanic & Atmospheric Administration (NOAA) [4]. Annual climatological summaries were downloaded for NOAA observation stations in Ames, Iowa (IA) (5 SE, #130203/99999); Roanoke, Virginia (VA) (Roanoke-Woodrum Airport, #447285/13741); and San Diego, California (CA) (Lindbergh Field, #047740/23188). Total precipitation was reported in inches per month. Histograms of monthly precipitation at each location were constructed in Minitab®. The lognormal distribution was found to be the best fit for each monthly precipitation dataset on the basis of Anderson-Darling statistics.

*1.2.4 Evaporation*

Daily water losses via evaporation from open pond surfaces were computed for each selected geographic location using the Penman Equation, Equation S1.

$$E = \frac{\Delta R_n + \gamma \times \lambda_v \times \rho_w \times K_E \times \nu_A \times (e_s^{\circ} - e_a)}{\lambda_v \times \rho_w \times (\Delta + \gamma)} \qquad \text{Eq S1.}$$

Where $E$ is daily evaporation depth (m/day), $\Delta$ is slope of the saturated vapor pressure vs. temperature relationship at daily average air temperature (kPa/˚C); $R_N$ is net solar radiation (MJ/m$^2$-d), $\gamma$ is psychrometric constant (≈ 0.066 kPa/˚C); $\lambda_v$ is latent heat of vaporization for water (2.45 MH/kg); $\rho_W$ is density of water (1000 kg/m$^3$); $K_E$ is a mass transfer coefficient (≈ 1.39E-8 kPa$^{-1}$); $\nu_A$ is wind speed (m/day); $e_S^{\circ}$ is saturation vapor pressure at atmospheric temperature (kPa); and $e_a$ is atmospheric water vapor pressure (kPa).

The slope of the saturated vapor pressure vs. temperature curve, $\Delta$, is given by the derivative summarized in Equation S2. Saturation vapor pressures at various temperatures were taken from Perry's Chemical Engineering Handbook [5]. $T$ is average daily temperature as taken from NSRDB.

$$\Delta = \frac{de^0}{dt}(0.625 \times exp(0.064 \times T)) = 0.04 \times exp(0.064 \times T) \qquad \text{Eq. S2}$$

Net solar radiation, $R_N$, was computed using the formulation given by Equation S3. Use of this equation as written required $G$ to be in units of W/m$^2$. Thus, values of daily global solar radiation, as downloaded from the NSRB, were divided by 24 h/d to convert from Wh/m$^2$.

$$R_N = 0.63 \times G - 40 \qquad \text{Eq. S3}$$

The quantity ($e_S^{\circ}$ - $e_a$) was computed using an empirical relationship for saturation vapor pressure ($e_s^{\circ}$) as a function of average daily temperature ($T$) [5] and daily measurements of relative humidity ($RH$) from the NSRB. Note that relative humidity values were expressed as fractions rather than percentages. This formulation is summarized in Equation S4.

$$e_s^{\circ} - e_a = 0.625\,exp(0.064 \times T) - 0.625\,exp(0.064 \times T) \times RH \qquad \text{Eq. S4}$$

Monthly evaporation was computed via multiplication of the average daily evaporation depths resulting from Equation S1 by the number of days in each month. These values were stochastic in so far as they

were computed by Crystal Ball via sampling from distributions for insolation, daily temperature, wind speed, and relative humidity.

### *1.2.5 Evapotranspiration*

Daily water losses via evapotranspiration from cultivated fields were computed for each selected geographic location using the Penman-Monteith Equation. Specifically, the so-called "standardized" method promulgated by the American Society of Civil Engineers' Environmental & Water Resources Initiative (ASCE-EWRI) was used to compute evapotranspiration during cultivation of corn, canola, and switchgrass [6]. This formulation is Equation S5.

$$ET = \frac{0.408\Delta \times (R_N - G_S) + \gamma \frac{Cn}{T+273} \times \nu_A \times (e_s^0 - e_a)}{\Delta + \gamma(1 + C_d \nu_A)} \qquad \text{Eq. S5}$$

Here, $ET$ is daily evapotranspiration depth (m/day); $G_S$ is soil heat flux density at the soil surface (MJ/m$^2$), $C_n$ and $C_d$ are ASCE-standardized coefficients for selected "reference" crops. Other parameters ($\Delta$, $R_N$, $\gamma$, $T$, $\nu_A$, $e_s^\circ - e_a$) are as defined for use in the Penman Equation (Equation S1). Corn, canola, and switchgrass were modeled using standardized coefficients for the "tall" reference crop ($C_n$ = 1600, $C_d$ = 0.38) [7].

Average daily $G_S$ values were computed using ASCE-standardized coefficients for daylight and nighttime soil heat fluxes. Daily hours of daylight ($t_{DAY}$) and darkness ($t_{NIGHT}$) over the course of a single year at each selected location were taken from data tabulated by the US Naval Observatory [8]. These values were incorporated into computation of $G_S$ as a function of daily net radiation ($R_N$) according to Equation S6.

$$G_S = \frac{R_N}{24} \times (0.04 t_{DAY} - 0.2 t_{NIGHT}) \qquad \text{Eq. S6}$$

Monthly evapotranspiration was computed via multiplication of the average daily evapotranspiration depths resulting from Equation S6 by the number of days in each month.

### *1.2.6 Summary*

Climactic inputs to the biomass production model include photosynthetically active radiation (PAR), temperature, wind speed, relative humidity, and precipitation. Input distributions for PAR, wind speed, and relative humidity were normally distributed; monthly precipitation was lognormally distributed. Averages ($\mu$) and standard deviations ($\sigma$) for distributions are summarized in Table S1. Crystal Ball was used to sample from the input climactic distributions for each of the months in one year. Evapotranspiration and evaporation at each location were then computed as model outputs. These two outputs were generally well fit by the gamma distribution for each of the selected geographic locations. Table S1 summarizes scale ($\theta$) and shape (k) factors corresponding to monthly best-fit gamma distributions for evaporation and evapotranspiration in each of the three selected geographic locations.

**Table S1.** Summarizes parameters used to form distributions of climactic model inputs (PAR, temperature, wind speed, relative humidity, precipitation) and outputs (evaporation and evapotranspiration). Tabulated values represent averages ($\mu$) and standard deviations ($\sigma$), using $\mu/\sigma$ notation, for normal/lognormal-distributed inputs or scale ($\theta$) and shape (k) parameters, using $\theta$/k notation, for gamma-distributed outputs. It should be noted that evaporation and evapotranspiration for months outside of each crop's respective growing season in a particular location are marked 'NA' for "not applicable".

| Average Photosynthetically Active Radiation (PAR) (MJ/m$^2$-day) | | | | | | | | | | | | |
|---|---|---|---|---|---|---|---|---|---|---|---|---|
| | Jan | Feb | Mar | Apr | May | Jun | Jul | Aug | Sep | Oct | Nov | Dec |
| CA | 5.0/0.4 | 6.3/0.5 | 8.0/0.6 | 9.9/0.5 | 10.1/0.8 | 10.5/0.9 | 11.2/0.6 | 10.6/0.5 | 8.8/0.6 | 7.1/0.4 | 5.5/0.3 | 4.6/0.3 |
| VA | 3.7/0.3 | 5.0/0.4 | 6.7/0.5 | 8.4/0.8 | 9.4/0.5 | 10.0/0.6 | 9.6/0.7 | 8.8/0.5 | 7.3/0.6 | 5.9/0.4 | 4.0/0.4 | 3.3/0.2 |
| IA | 3.0/0.2 | 4.4/0.3 | 6.0/0.5 | 7.6/0.6 | 9.3/0.6 | 10.3/0.6 | 10.2/0.6 | 8.9/0.5 | 6.9/0.6 | 4.9/0.4 | 3.0/0.2 | 2.5/0.2 |
| Average Daily Temperature Per Month (° C) | | | | | | | | | | | | |
| | Jan | Feb | Mar | Apr | May | Jun | Jul | Aug | Sep | Oct | Nov | Dec |
| CA | 14.1/1.3 | 14.8/1.3 | 15.3/1.1 | 16.7/1.1 | 17.8/1.0 | 19.3/1.3 | 21.6/1.3 | 22.5/1.1 | 21.9/1.5 | 19.9/1.0 | 16.6/1.0 | 14.1/1.3 |
| VA | 1.4/2.7 | 2.9/2.1 | 8.2/1.9 | 13.1/1.5 | 17.8/1.5 | 22.0/1.1 | 24.2/1.0 | 23.7/1.0 | 19.8/1.3 | 13.6/1.8 | 8.6/1.6 | 3.5/2.4 |
| IA | -10.4/3.8 | -7.4/3.2 | -0.3/3.2 | 8.0/2.0 | 14.8/2.0 | 20.2/1.5 | 22.5/1.3 | 21.0/1.4 | 16.0/1.2 | 9.6/2.1 | 1.1/2.1 | -7.6/3.3 |
| Average Daily Wind Speed (m/s) | | | | | | | | | | | | |
| | Jan | Feb | Mar | Apr | May | Jun | Jul | Aug | Sep | Oct | Nov | Dec |
| CA | 2.7/0.4 | 3.0/0.4 | 3.5/0.3 | 3.7/0.2 | 3.6/0.2 | 3.6/0.2 | 3.5/0.2 | 3.5/0.2 | 3.4/0.2 | 3.1/0.2 | 2.8/0.3 | 2.6/0.4 |
| VA | 4.2/0.6 | 4.2/0.6 | 4.4/0.6 | 4.3/0.5 | 3.6/0.4 | 3.0/0.4 | 3.1/0.4 | 2.7/0.3 | 2.8/0.4 | 3.1/0.4 | 3.7/0.6 | 3.8/0.6 |
| IA | 5.8/0.5 | 5.5/0.6 | 5.8/0.5 | 5.8/0.5 | 5.3/0.5 | 4.8/0.4 | 3.9/0.4 | 3.7/0.4 | 4.2/0.5 | 4.8/0.5 | 5.3/0.6 | 5.4/0.6 |
| Average Relative Humidity (%) | | | | | | | | | | | | |
| | Jan | Feb | Mar | Apr | May | Jun | Jul | Aug | Sep | Oct | Nov | Dec |
| CA | 63/6 | 66/6 | 67/4 | 67/4 | 71/3 | 74/3 | 75/3 | 74/3 | 73/4 | 69/6 | 66/7 | 64/7 |
| VA | 61/5 | 60/7 | 57/7 | 57/7 | 66/4 | 69/5 | 71/5 | 73/4 | 74/5 | 68/6 | 65/7 | 64/5 |
| IA | 74/7 | 77/6 | 76/6 | 68/6 | 65/6 | 67/5 | 73/5 | 76/4 | 76/6 | 72/6 | 78/5 | 79/5 |
| Average Monthly Precipitation (cm/month) | | | | | | | | | | | | |
| | Jan | Feb | Mar | Apr | May | Jun | Jul | Aug | Sep | Oct | Nov | Dec |
| CA | 5.7/5.9 | 5.8/4.7 | 5.1/4.9 | 1.9/1.9 | 0.4/0.6 | 0.2/0.5 | 0.1/0.2 | 0.1/0.2 | 0.4/0.7 | 1.3/2.4 | 2.5/2.7 | 3.7/3.0 |
| VA | 7.6/4.9 | 7.5/4.4 | 8.9/4.6 | 9.0/5.6 | 9.7/5.1 | 9.9/6.7 | 10.1/5.1 | 8.8/5.4 | 9.9/8.4 | 7.5/5.7 | 8.2/5.7 | 6.7/3.1 |
| IA | 0.9/0.5 | 0.3/0.6 | 2.2/1.5 | 3.3/1.9 | 4.7/2.4 | 5.0/3.1 | 4.8/3.1 | 4.7/3.1 | 3.1/1.5 | 2.5/1.6 | 2.3/1.6 | 1.2/0.8 |
| Average Monthly Evaporation (mm/month) | | | | | | | | | | | | |
| | Jan | Feb | Mar | Apr | May | Jun | Jul | Aug | Sep | Oct | Nov | Dec |
| CA | 1.1/41.8 | 1.1/42.3 | 1.2/47.4 | 0.9/78.8 | 1.4/50.3 | 1.7/48.1 | 1.1/68.9 | 0.9/73.2 | 1.3/49.9 | 1.0/59.4 | 1.0/45.8 | 1.1/34.7 |
| VA | 1.2/27.7 | 1.3/30.4 | 1.6/36.3 | 1.8/43.4 | 1.2/56.2 | 1.2/62.5 | 1.5/52.6 | 0.9/67.1 | 1.3/42.1 | 1.2/42.8 | 1.2/37.4 | 1.0/29.8 |
| IA | NA | NA | NA | 1.8/36.5 | 1.8/47.2 | 1.5/58.7 | 1.3/60.7 | 1.2/56.3 | 1.4/41.1 | 1.4/33.5 | 0.8/31.4 | NA |
| Average Monthly Evapotranspiration (mm/month) | | | | | | | | | | | | |
| | Jan | Feb | Mar | Apr | May | Jun | Jul | Aug | Sep | Oct | Nov | Dec |
| CA | NA | NA | NA | 1.9/56.9 | 1.7/54.5 | 1.9/47.3 | 1.7/58.2 | 1.5/64.1 | 2.1/48.7 | NA | NA | NA |
| VA | NA | NA | NA | NA | 2.5/46.3 | 2.4/49.3 | 2.7/49.6 | 1.9/54.6 | 2.2/41.5 | NA | NA | NA |
| IA | NA | NA | NA | NA | 3.9/35.8 | 3.4/42.2 | 3.1/42.2 | 2.5/41.3 | 3.0/35.5 | NA | NA | NA |

Anderson-Darling (A-D) statistics for the distributions referenced in Table S1 are summarized in Table S2. These values indicate the extent to which each climactic input is well fit by the selected statistical distribution. Recall that PAR, temperature, wind speed, and relative humidity were fit to normal distributions. Precipitation was fit to the lognormal distribution. Lower values of the A-D statistic indicate better fits. In general, and for the normal distribution in particular, A-D values less than 1.5 are said to be indicative of a reasonably well-fit distribution.

Table S2. Summarizes Anderson-Darling statistics (goodness-of-fit) for selected climactic input distributions. All parameters were fit to the normal distribution except monthly precipitation, which was fit to the lognormal distribution. Asterisks (**) indicate distributions for which an Anderson-Darling statistic could not be computed.

| Average Photosynthetically Active Radiation (PAR) – Normal Distribution | | | | | | | | | | | | |
|---|---|---|---|---|---|---|---|---|---|---|---|---|
| | Jan | Feb | Mar | Apr | May | Jun | Jul | Aug | Sep | Oct | Nov | Dec |
| CA | 0.76 | 0.33 | 0.67 | 0.46 | 0.25 | 0.52 | 0.84 | 0.65 | 0.81 | 0.24 | 0.24 | 0.22 |
| VA | 0.32 | 0.29 | 0.22 | 0.42 | 0.44 | 0.51 | 0.16 | 0.37 | 0.45 | 0.71 | 0.58 | 0.24 |
| IA | 0.23 | 0.36 | 0.41 | 0.21 | 0.48 | 0.16 | 0.21 | 0.25 | 0.20 | 0.19 | 0.63 | 0.34 |
| Average Daily Temperature Per Month – Normal Distribution | | | | | | | | | | | | |
| | Jan | Feb | Mar | Apr | May | Jun | Jul | Aug | Sep | Oct | Nov | Dec |
| CA | 1.38 | 0.43 | 0.38 | 0.46 | 0.56 | 0.49 | 0.52 | 0.49 | 0.63 | 0.26 | 0.28 | 0.50 |
| VA | 0.31 | 0.76 | 0.48 | 0.18 | 0.30 | 0.40 | 0.59 | 1.34 | 0.34 | 0.20 | 0.29 | 0.24 |
| IA | 0.22 | 0.56 | 0.43 | 0.22 | 0.45 | 0.65 | 0.22 | 0.34 | 0.20 | 0.27 | 0.49 | 0.23 |
| Average Daily Wind Speed – Normal Distribution | | | | | | | | | | | | |
| | Jan | Feb | Mar | Apr | May | Jun | Jul | Aug | Sep | Oct | Nov | Dec |
| CA | 0.18 | 0.42 | 0.50 | 0.57 | 1.26 | 0.46 | 0.35 | 0.52 | 0.38 | 0.46 | 0.37 | 0.23 |
| VA | 0.31 | 0.76 | 0.48 | 0.18 | 0.30 | 0.40 | 0.59 | 1.34 | 0.34 | 0.20 | 0.29 | 0.24 |
| IA | 0.43 | 0.22 | 0.28 | 0.42 | 0.37 | 0.23 | 0.68 | 0.28 | 0.51 | 0.17 | 0.37 | 0.31 |
| Average Relative Humidity – Normal Distribution | | | | | | | | | | | | |
| | Jan | Feb | Mar | Apr | May | Jun | Jul | Aug | Sep | Oct | Nov | Dec |
| CA | 0.40 | 0.63 | 0.21 | 0.50 | 0.55 | 0.51 | 0.36 | 1.10 | 1.18 | 0.25 | 0.39 | 0.49 |
| VA | 0.36 | 0.57 | 0.25 | 0.46 | 0.27 | 0.23 | 0.55 | 0.25 | 0.36 | 0.33 | 0.36 | 0.40 |
| IA | 0.44 | 0.47 | 1.04 | 0.30 | 0.23 | 0.25 | 0.40 | 0.44 | 0.21 | 0.26 | 0.36 | 0.37 |
| Average Monthly Precipitation (cm/month) – Lognormal Distribution | | | | | | | | | | | | |
| | Jan | Feb | Mar | Apr | May | Jun | Jul | Aug | Sep | Oct | Nov | Dec |
| CA | 0.40 | 0.52 | ** | ** | ** | ** | ** | ** | ** | ** | ** | 1.44 |
| VA | 0.31 | 0.42 | 0.69 | 0.33 | 0.41 | 0.52 | 0.37 | 0.19 | 0.53 | 2.22 | 1.22 | 0.94 |
| IA | 1.97 | 1.61 | 0.89 | 0.52 | 0.98 | 0.26 | 0.51 | 1.00 | 0.44 | 0.76 | 1.41 | 1.36 |

## 1.3 Crop Yield Estimates

### *1.3.1 Corn*

Silage corn yield estimates were computed on the basis of growing season insolation and empirical estimates of radiation-use efficiency (RUE). RUE is the amount of aboveground crop biomass produced per unit PAR flux. Each location was assumed to have the same annual growing season for corn: 1 May – 15

September. Biomass was assumed to be 35-42% dry matter at harvest, and this value was modeled using a uniform distribution over the given range [9].

The methodology of Kiniry et al (1989) was used to estimate corn yields (Mg/ha) at each location according to Equation S7 [10].

$$Yield_{CORN} = RUE_{CORN} \times \sum (IPAR) = RUE_{CORN} \times \sum PAR \times (1 - e^{-k \times LAI}) \qquad \text{Eq. S7}$$

IPAR is intercepted photosynthetically active radiation. This can be measured directly or computed as a function of extinction coefficient (k = 0.65) and leaf area index (LAI). Values of dimensionless LAI were taken from the literature and found to be normally distributed with average = 4.59 and standard deviation = 0.43 (n = 12) [11]. Average monthly IPAR values were summed over the growing season to compute cumulative IPAR at each location. Values of $RUE_{CORN}$, in units of grams dry biomass per MJ IPAR, were taken from the literature and found to be lognormally distributed with average = 3.46 and standard deviation = 0.80 (n = 37; Anderson-Darling = 1.4) [10]. $RUE_{CORN}$ was multiplied by the cumulative IPAR at each location to estimate annual corn yields at each location. Resulting estimates of annual corn yield at each location were lognormally distributed. Resulting average estimates were also compared to literature values and found to be consistent with reported ranges. Pertinent distribution parameters and distribution goodness-of-fit are summarized in Table S3.

**Table S3.** Cumulative intercepted photosynthetically active radiation (IPAR) and average estimated wet yields ($\mu$) (with standard deviations, $\sigma$) for corn production in three geographic locations. Low values of the Anderson-Darling (A-D) statistic indicate that each wet yield distribution is well fit by the lognormal distribution; average estimates are well-aligned with previous measurements as indicated at far right.

| Location | Average Cumulative IPAR ($MJ/m^2$) | Estimated Wet Yield $\mu/\sigma$ (Mg/ha) | Lognormal Distribution A-D Statistic | Average Measured Wet Yield (Mg/ha) [Source] |
|---|---|---|---|---|
| CA | 1364 | 47.2/11.0 | 0.14 | 45 – 68 [12] |
| VA | 1209 | 45.5/10.7 | 0.55 | 32 – 56 [9] |
| IA | 1228 | 42.5/9.9 | 0.41 | 39 – 50 [13] |

### *1.3.2 Switchgrass*

Switchgrass yield estimates for each of the selected locations were computed on the basis of growing season insolation and radiation use efficiency using an empirically derived estimate of $RUE_{SGRASS}$. Data for several types of switchgrass and several geographic locations within the US were used to compute an estimate for $RUE_{SGRASS}$ in units of grams aboveground dry biomass per MJ PAR. Cultivars included lowland varieties 'Alamo' and 'Kanlow' as well as upland cultivars 'Cave-in-Rock', and 'Shelter'. Yield measurements for these varieties were measured in the following locations: Princeton, KY; Raleigh, NC; State College, PA; Jackson and Knoxville, TN; Roanoke, VA (two test plots); and, Morgantown, WV [14, 15]. RUE was computed as the ratio between dry switchgrass yield and measurements of PAR as taken from the NSRDB for each of these six locations. Switchgrass growing season was assumed to be 1 May – 1 Aug for each of these locations except State College, PA, where it was 1 June – 1 September. Pertinent information is summarized in Table S4.

**Table S4.** Photosynthetically active radiation (PAR) [2], reported wet switchgrass yields, and computed radiation use efficiency (RUE) values for switchgrass production in several geographic regions [15, 16].

| Location | Year | PAR ($MJ/m^2$) | Yield (Mg/ha) | RUE (g/MJ) |
|---|---|---|---|---|
| Jackson, TN | 2000 | 920 | 8.8 | 0.96 |
| | 2001 | 913 | 10.3 | 1.13 |
| Knoxville, TN | 2000 | 931 | 15.6 | 1.68 |
| | 2001 | 868 | 18.1 | 2.09 |
| Morgantown, WV | 2000 | 847 | 15.1 | 1.78 |
| | 2001 | 866 | 17.8 | 2.06 |
| Princeton, KY[a] | 2000 | 885 | 12.6 | 1.42 |
| | 2001 | 914 | 13.1 | 1.43 |
| Raleigh, NC | 2000 | 878 | 12.1 | 1.38 |
| | 2001 | 877 | 6.4 | 0.73 |
| Roanoke, VA | 2000 | 849 | 15.7 | 1.85 |
| | 2000 | 876 | 13.1 | 1.50 |
| | 2001 | 852 | 15.6 | 1.83 |
| | 2001 | 869 | 15.4 | 1.77 |
| State College, PA | 2002 | 904 | 7.9 | 1.06 |
| | 2003 | 802 | 7.0 | 1.02 |
| | 2004 | 800 | 7.0 | 1.07 |

[a] PAR data are from nearest NSRDB station in Evansville, IN.

$RUE_{SGRASS}$ values in Table S4 were fit to the lognormal distribution, using average = 1.46 g/MJ and standard deviation = 0.41 (n = 17; Anderson-Darling = 0.42). Switchgrass yields in CA, IA, and VA were then estimated by computing cumulative PAR over each area's growing season and multiplying that number by the empirical estimate of $RUE_{SGRASS}$. Growing seasons were assumed to be 1 May – 1 August in Virginia, 1 June – 1 September in Iowa, and 1 April – 16 September in California. Resulting annual switchgrass yields were found to be lognormally distributed in each location, and mean values were benchmarked against published reports. This data is summarized in Table S5.

**Table S5.** Cumulative photosynthetically active radiation (PAR) and average estimated wet yields ($\mu$) (with standard deviation, $\sigma$) for switchgrass growing seasons in three geographic locations. Low values of the Anderson-Darling (A-D) statistic indicate that each wet yield distribution is well fit by the lognormal distribution; estimates are consistent with previous measurements as indicated at far right.

| Location | Average Cumulative PAR ($MJ/m^2$) | Estimated Wet Yield $\mu/\sigma$ (Mg/ha) | Lognormal Distribution A-D Statistic | Average Measured Wet Yield (Mg/ha) [Source] |
|---|---|---|---|---|
| CA | 1733 | 25.2/7.1 | 0.21 | 22.5 – 33.8 [17] |
| VA | 890 | 12.9/3.7 | 0.35 | 4.0 – 15.0 [9, 15] |
| IA | 900 | 13.1/3.8 | 0.27 | 4.5 – 14.4 [18] |

### *1.3.3 Canola*

Estimates of canola dry yield were computed for each of the selected locations on the basis of growing season insolation and radiation use efficiency using an empirically derived estimate of $RUE_{CANOLA}$. Data for several types of winter canola and several geographic locations within the US were used to compute an estimate for $RUE_{CANOLA}$ in units of grams aboveground dry biomass per MJ PAR. Cultivars included those utilized in the 2003 National Winter Canola Variety Trial (NWCVT) [Rife et al, 2003] and others. Yield measurements were taken from selected NWCVT locations plus Corvallis, OR; Marianna, AR;

Othello, WA; and Pendleton, OR [14, 15]. RUE was computed as the ratio between dry seed yield as published in literature reports [19, 20] and measured PAR as taken from the NSRDB for each of these locations. Canola growing seasons were taken from the respective literature reports [19, 20]. Pertinent information is summarized in Table S6.

**Table S6.** Summarizes photosynthetically active radiation (PAR) [21], reported winter canola seed yields, and computed radiation use efficiency (RUE) values for several geographic regions in the US.

| Location | Year | Growing Season | PAR ($MJ/m^2$) | Yield (Mg/ha) | RUE (g/MJ) |
|---|---|---|---|---|---|
| Belleville, IL | 2002-2003* | 25 Sep – 25 Jun | 1607 | 3707 | 0.23 |
| Columbia City, IN | 2002-2003* | 12 Sep – 17 Jul | 3852† | 1081 | 0.03 |
| Corvallis, OR | 2004-2005 | 1 Sep – 1 Jul | 1481 | 4324 | 0.29 |
| Garden City, KS | 2002-2003* | 6 Sep – 1 Jul | 2077 | 1836 | 0.09 |
| Griffin, GA | 2002-2003* | 3 Oct – 6 Jun | 1644 | 1849 | 0.11 |
| Kibler, AR | 2002-2003* | 3 Oct – 17 Jun | 1614† | 1858 | 0.12 |
| Lexington, KY | 2002-2003* | 25 Sep – 23 Jun | 1381 | 2570 | 0.19 |
| Lincoln, NE | 2002-2003* | 10 Sep – 10 Jul | 1926 | 3285 | 0.17 |
| Marianna, AR | 2001-2002 | 15 Oct – 15 Jun | 1685† | 3131 | 0.25 |
| | 2003-2004 | 15 Oct – 15 Jun | 1534† | 4102 | 0.27 |
| Meridianville, AL | 2002-2003* | 4 Oct – 10 Jun | 1484† | 1269 | 0.09 |
| Munday, TX | 2002-2003* | 23 Sep – 4 Jun | 1696† | 413 | 0.02 |
| Novelty, MO | 2002-2003* | 2 Sep – 3 Jul | 1786† | 2047 | 0.12 |
| Orange, VA | 2002-2003* | 25 Sep – 26 Jun | 1419† | 2995 | 0.27 |
| Othello, WA | 2007-2008 | 10 Sep – 23 Jul | 1802† | 5064 | 0.28 |
| Pendleton, OR | 2001-2002 | 1 Sep – 1 Jul | 1685 | 3131 | 0.17 |
| | 2002-2003 | 1 Sep – 1 Jul | 1718 | 2706 | 0.16 |
| | 2004-2005 | 1 Sep – 1 Jul | 1698 | 2858 | 0.19 |
| Torrington, WY | 2002-2003* | 26 Aug – 21 Jul | 2296† | 1977 | 0.09 |

* Indicates investigation conducted as part of 2003 National Winter Canola Variety Trial (NWCVT).

† Indicates location for which PAR data was not directly available from NSRDB so closest observation station was used instead. Columbia City, IN = Fort Wayne, IN; Griffin, GA = Atlanta, GA; Kibler, AR = Fort Smith, AR; Marianna, AR = Stuttgart, AR; Meridianville, AL = Hunstville, AL; Munday, TX = Wichita Falls, TX; Novelty, MO = Kirkville, MO; Orange, VA = Charlottesville, VA; Othello, WA = Ephrata, WA; Torrington, WY = Scottsbluff, NE.

$RUE_{CANOLA}$ values in Table S6 were fit to the lognormal distribution, using average = 0.164 g/MJ and standard deviation = 0.084 (n = 19; Anderson-Darling = 0.86). Although the normal distribution exhibited a lower Anderson-Darling statistic, and thus a better fit for this data, the lognormal data was used to ensure that sampled values of $RUE_{CANOLA}$ were never less than zero. Winter canola seed yield at each selected geographic location was estimated by computing cumulative PAR over each area's growing season and multiplying that number by $RUE_{CANOLA}$. Resulting estimates for wet seed yield were multiplied by 0.92 to account for the fact that canola seeds are roughly 8% moisture by mass before drying. Dry seed masses were then multiplied by a factor of three to account for the mass of stalks and pods, since canola seeds comprise 1/3 of the plant's dry weight while stalks and pods account for the other 2/3 [22]. Growing seasons were assumed to be 1 September– 30 June in Virginia [23, 24], 15 September – 15 July in Iowa (based on similarity in latitude and weather conditions among Ames, IA; Columbia City, IN; and

Lincoln, NE) [23] and 15 October – 30 May in California [25, 26]. Resulting annual canola yields were found to be lognormally distributed in each location, and mean values were benchmarked against published reports. This data is summarized in Table S7.

**Table S7.** Summarizes cumulative photosynthetically active radiation (PAR) and average dry yields ($\mu$) (with standard deviation, $\sigma$) for winter canola growing seasons in three geographic locations. Yields represent total biomass; i.e. seeds plus stalks. Low values of the Anderson-Darling (A-D) statistic indicate that each dry yield distribution is well fit by the lognormal distribution. Average estimates are well aligned with previously measured dry yields as indicated at far right. Previously reported values for canola seed yield have been multiplied by three to reflect the assumption that seeds account for 1/3 of canola's weight while straw and pods (i.e., stover) account for the other 2/3.

| Location | Average Cumulative PAR ($MJ/m^2$) | Estimated Total Dry Yield $\mu/\sigma$ (Mg/ha) | Lognormal Distribution A-D Statistic | Average Measured Total Dry Yield (Mg/ha) [Source] |
|---|---|---|---|---|
| CA | 1608 | 7.1/0.7 | 0.23 | 6.4 – 13.3 [25, 26] |
| VA | 1933 | 8.5/0.9 | 0.36 | 6.6 – 9.0 [23, 24] |
| IA | 1810 | 7.8/0.8 | 0.40 | 3.2 – 9.8 [23] |

### *1.3.4 Algae*

Algae dry yield estimates for each of the selected locations were computed on the basis of growing season insolation and radiation use efficiency using an empirically derived estimate of $RUE_{ALGAE.}$ This estimate was derived from literature reports of field-scale algae cultivation in open ponds by Benemann & Oswald (1996), Kadam (2001), and Weissmann & Tillet (1992) [3, 27, 28]. Their ponds were operated in Brawley, CA; San Juan, NM; and, Roswell, NM, respectively. Table S8 summarizes average estimated monthly yields reported by the authors and average monthly PAR values as taken from the NSRDB for stations located closest to each area of interest: San Diego, CA for Brawley, CA; Albuquerque, NM for San Juan, NM; and, Tucumcari, NM for Roswell, NM.

**Table S8.** Summarizes reported and estimated monthly values of radiation use efficiency for pilot-scale algae production in three different locations.

| Month | Brawley, CA [San Diego, CA] | | | Roswell, NM [Tucumcari, NM] | | | San Juan, NM [Albuquerque, NM] | | | Mean RUE (g/MJ) |
|---|---|---|---|---|---|---|---|---|---|---|
| | Yield (Mg/ha) | PAR ($MJ/m^2$) | RUE (g/MJ) | Yield (Mg/ha) | PAR ($MJ/m^2$) | RUE (g/MJ) | Yield (Mg/ha) | PAR ($MJ/m^2$) | RUE (g/MJ) | |
| Jan | 93 | 154 | 0.6 | 90 | 150 | 0.6 | | | | 0.64 |
| Feb | 112 | 176 | 0.6 | 112 | 178 | 0.6 | | | | 0.63 |
| Mar | 217 | 248 | 0.9 | 254 | 255 | 1.0 | | | | 1.13 |
| Apr | 360 | 297 | 1.2 | 111 | 310 | 0.4 | | | | 0.83 |
| May | 527 | 314 | 1.7 | 270 | *351* | 0.8 | *973* | 387 | 2.5 | 1.26 |
| Jun | 600 | 314 | 1.9 | 420 | *362* | 1.2 | *942* | 393 | 2.4 | 1.89 |
| Jul | 620 | 348 | 1.8 | 614 | *361* | 1.7 | *973* | 379 | 2.6 | 1.99 |
| Aug | 620 | 328 | 1.9 | 564 | *32* | 1.7 | *973* | 346 | 2.8 | 2.09 |
| Sep | 690 | 264 | 2.6 | 474 | *267* | 1.8 | *942* | 285 | 3.3 | 2.40 |
| Oct | 682 | 221 | 3.1 | 419 | *225* | 1.9 | *973* | 237 | 4.1 | 2.78 |
| Nov | 90 | 166 | 0.5 | 141 | 158 | 0.9 | | | | 1.85 |
| Dec | 93 | 143 | 0.6 | 71 | 137 | 0.5 | | | | 0.57 |

Two of the three studies summarized in Table S8 reported measured yields for each month of the calendar year. In contrast, Kadam (2002) reported only average photosynthetic efficiency, 4.86% on PAR basis over one year [29]. He also reported a total pond area of 1000 ha, estimated daily dry yield of 314,300 kg, and 250 operational days per year. These figures were thus used to back-calculate corresponding $RUE_{ALGAE}$ values for each month. First, daily yield of 314,300 kg in a 1000 ha pond corresponds to 31.4 $g/m^2$-day productivity. This value was multiplied by the number of days per month to yield estimates of monthly yields. These figures are shown in italicized font within Table S8. In dividing the estimated monthly yields by measured values of average monthly PAR, it was possible to compute estimates of average monthly $RUE_{ALGAE}$. Kadam's overall photosynthetic efficiency was then converted from PAR basis to biomass basis by multiplying 4.86% by the molecular weight of glucose (180 g/mole) and dividing by its energy content (2.87 MJ/mole glucose). This yielded an average annual RUE of 3.0 g/MJ. It was then possible to select the 250-day combination of monthly averages exhibiting this overall RUE average, namely 1 May – 31 Oct. The resulting back-calculated values of $RUE_{ALGAE}$ in each of these months for Roswell, NM are indicated in Table S8.

Taken together with the monthly $RUE_{ALGAE}$ values from Brawley, CA and Roswell, NM, the back-calculated values for San Juan, NM were used to formulate triangular distributions for monthly $RUE_{ALGAE}$ values during May – October. For months not sampled within the Kadam study (November – April), uniform distributions were assumed to cover the range between values reported by the other two studies [3, 28]. Annual algae yields at the selected geographic locations were then computed by multiplying each month's PAR value by its associated monthly $RUE_{ALGAE}$ estimate. These products were then summed over an entire year. Algae cultivation was assumed to be impossible in months with an average daily temperature less than 0 °C [28]. As such, Iowa yields for the months of January, February, March, and December were assigned a value of zero. Resulting estimates of annual algae yield in each location were normally distributed. Table S9 summarizes annual algae yields at each location.

**Table S9.** Summarizes cumulative photosynthetically active radiation (PAR) and average estimated dry algae yields ($\mu$) (with standard deviation, $\sigma$) for three geographic locations. Low values of the Anderson-Darling (A-D) statistic indicate that each yield distribution is well fit by the normal distribution.

| Location | Average Cumulative PAR ($MJ/m^2$) | Estimated Dry Yield $\mu/\sigma$ (Mg/ha) | Normal Distribution A-D Statistic |
|---|---|---|---|
| CA | 1733 | 47.1/2.5 | 0.87 |
| VA | 890 | 40.2/2.2 | 0.35 |
| IA | 900 | 34.5/2.1 | 0.27 |

Figures S1 – S3 summarize predicted values of algae dry yield for each month of the year in three geographic locations of interest. Yield estimates from previously published sources are also presented in each figure for point of reference.

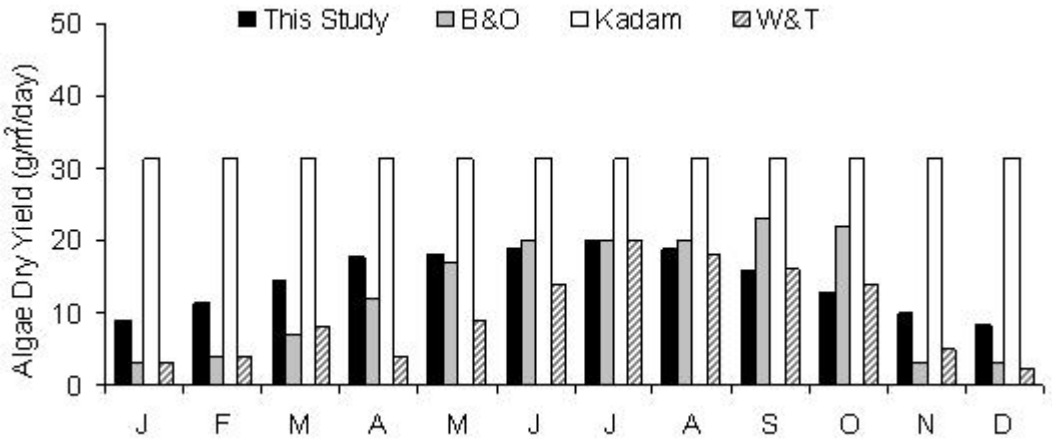


Figure S1. Estimated algae dry yields by month in San Diego, CA. Yield estimates reflect reported $RUE_{ALGAE}$ values from various sources (B&O = Benemann & Oswald (1996) [3]; Kadam = Kadam (2002) [29]; W&T = Weissman and Tillett (1990) [28]) as multiplied by growing season PAR in San Diego, CA.

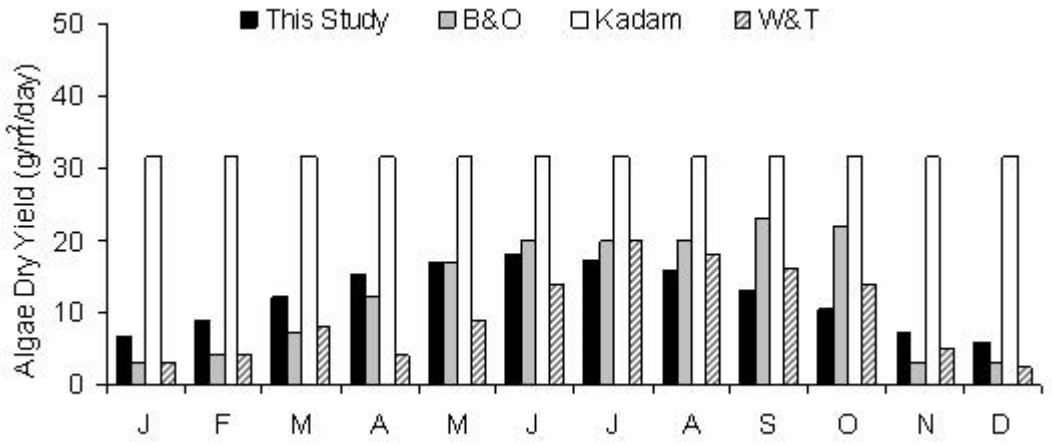


Figure S2. Estimated algae dry yields by month in Roanoke, VA. Yield estimates reflect reported $RUE_{ALGAE}$ values from various sources (B&O = Benemann & Oswald (1996) [3]; Kadam = Kadam (2002) [29]; W&T = Weissman and Tillett (1990) [28]) as multiplied by growing season PAR in Roanoke, VA.

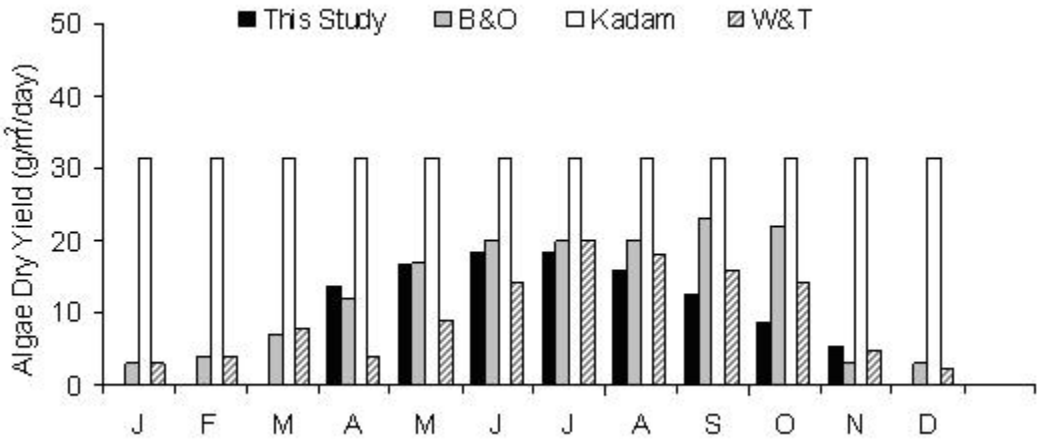


Figure S3. Estimated algae dry yields by month in Ames, IA. Yield estimates reflect reported $RUE_{ALGAE}$ values from various sources (B&O = Benemann & Oswald (1996) [3]; Kadam = Kadam (2002) [29]; W&T = Weissman and Tillett (1990) [28]) as multiplied by growing season PAR in Ames, IA.

### 1.4 Selection of Open Ponds v. Photobioreactors

The decision to model open ponds in this research is based primarily on the economics of biomass production for fuel and the likelihood that these reactors will be used in the near future. Recent research has focused on photobioreator design for optimal growth rates and in this regard, photobioreactors do offer certain benefits over open ponds: 1) higher cell densities can be obtained, and 2) pure cultures of lipid-rich organisms can be grown without risk of contamination by other species [30]. Despite these advantages, the cost of photobioreactors makes them highly unfavorable for energy production applications. Growing algae for fuel will require large-scale operations and the capital cost of photobioreactor projects increases linearly with production much faster than open ponds. One estimate is that cost of producing algae from photobioreactors is an order of magnitude higher than in open ponds [31]. Additionally, the land footprint of photobioreactors is not much better than open ponds. More importantly, the life cycle burdens of photobioreactors are expected to be many times higher than open ponds in terms of greenhouse gas emissions, energy use, and water use. The production of all the required materials (glass, metal, concrete foundations, etc) for production of a photobioreactor is expected make them an unfavorable option relative to open ponds. The primary contributions to the life cycle of algae, e.g., the nutrient use and $CO_2$ consumption, would not be changed regardless of the growing method. For this reason the open pond results reported here could be considered a 'best case' scenario for photobioreactors assuming the impacts from producing and operating the facility were offset by the improved productivity.

### 1.5 Algae Stoichiometry and Fertilizer Requirements

#### *1.5.1 Algae Stoichiometry*

The molecular composition of algae was used to help define several of the estimates used in this study including the $CO_2$ uptake rate, fertilizer addition rates, etc. The molecular composition of algae is largely consistent between photosynthetic species as demonstrated by Redfield [32].

$$\text{Algae} = C_{106}H_{181}O_{45}N_{15}P \text{ (MW = 2414)}$$

Production of algae biomass was assumed to proceed via the combination of carbon dioxide + water + urea + phosphate + light via the following chemical reaction:

$$99.5\ CO_2 + 75.5\ H_2O + 7.5\ CO(NH_2)_2 + ½\ P_2O_5 \rightarrow C_{106}H_{181}O_{45}N_{15}P + 119.75\ O_2 \qquad \text{Eq. S8}$$

This stoichiometry was utilized in estimating amounts of various required inputs for algae cultivation.

*1.5.2 Fertilizer Requirements*

A combination of literature data and algae stoichiometry, as defined in §1.5.1, were used to determine appropriate mass dosing for nitrogen (N) and phosphorus (P) fertilizers. Triangular distributions were used for both N and P dosing rates. Minimum, maximum, and most likely nitrogen concentrations were set to 23, 140, and 70 mg/L as N, respectively [33]. Minimum, maximum, and most likely phosphorus concentrations were set to 10, 102, and 29 mg/L as $P_2O_5$, respectively [33]. Use of these distributions led to N and P doses that were just less than 2× the stoichiometric requirements for the average computed algae yield. It was assumed that the excess N and P may be diverted to other biochemical reactions (e.g., production of extracellular material, bacterial growth, etc.). Since the water balance was assumed to be at steady-state, dose concentrations were multiplied by the amount of water centrifuged out of the system each month to compute total required masses of each nutrient per month. For all of the modeled scenarios, urea ($(NH_2)_2CO$) was used as N source and superphosphate ($Ca(H_2PO_4)_2$) was used as P source.

## 1.6 High Heating Values of Biomass Stocks

Data from the Energy research Centre of the Netherlands ECN was combined with results from our own literature review to compile a table of biomass compositions and high heating values (HHV) for the four types of biofeedstocks investigated in this study. Literature measurements of algae biomass HHV was confirmed in measurements performed by an algae start-up company located outside Richmond, VA. This firm estimates the HHV of dried algae to be 24300 kJ/kg. For biomass samples where HHV was not reported, the relationship between C-H-N embodied by Eq. S9 was used to formulate an estimate.

$$HHV\ (MJ/Mg) = 35160 \times wt\ \%\ C + 116225 \times wt\ \%\ H - 11090 \times wt\ \%\ O + 6280 \times wt\ \%\ N \qquad \text{Eq. S9}$$

HHV values taken from the literature or estimated using Eq. S9 were incorporated into triangular distributions using the minimum, maximum, and most likely values. For corn and canola, two separate triangular distributions were utilized for the grain (kernels or seed) and stover/straw. Composite HHV, encapsulating the amount of energy that would be released upon combustion of the entire plant, was then computed using a mass-weighed average of the kernel/seed and stover/straw HHVs for each plant. Each range of values summarized in Table S10 was fit to a triangular distribution according to HHV ~ Triangular (minimum value, likeliest value, and maximum value). HHV values for each type of biomass are summarized in Table S10.

**Table S10.** Summarizes approximate elemental composition (i.e., weight percentage comprising carbon, hydrogen, oxygen, and nitrogen) and high heating value (HHV) estimates for each of the biomass feedstocks evaluated in this investigation.

| Feedstock | C% | H% | O% | N% | HHV (MJ/Mg) | Source |
|---|---|---|---|---|---|---|
| Algae | 52.7 | 7.22 | 28.9 | 8.01 | 23480 | [35] |
| Algae | 43.9 | 6.86 | 34.5 | 6.54 | 19818 | [36] |
| Algae | 54.8 | 6.67 | 23.5 | 6.66 | 26357 | [35] |
| Algae | 52.7 | 7.22 | 28.9 | 8.01 | *24219 | [37] |
| Minimum HHV | | | | | 19800 | |
| Maximum HHV | | | | | 26400 | |
| Likeliest Value HHV | | | | | 24000 | |
| Switchgrass | 47.4 | 5.75 | 42.3 | 0.74 | 18641 | [38] |
| Switchgrass | 47.5 | 5.80 | 43.6 | 0.36 | 18559 | [38] |
| Switchgrass | 47.8 | 5.76 | 35.1 | 1.17 | 18024 | [39] |
| Switchgrass | 42 | 5 | 35 | 0.2 | *16710 | [40] |
| Minimum HHV | | | | | 16700 | |
| Maximum HHV | | | | | 18650 | |
| Likeliest Value HHV | | | | | 18300 | |
| Corn kernels | 44.6 | 5.37 | 39.6 | 0.41 | 17690 | [35] |
| Corn kernels | 44 | 6.4 | 49.2 | 1.1 | *17522 | [41] |
| Corn kernels | 43.4 | 6.17 | 45.8 | 1.02 | 17359 | [42] |
| Corn kernels | 42 | 5 | 42 | 0.7 | *15965 | [40] |
| Corn kernels | | | | | 15900 | [43] |
| Corn stover | 37.8 | 4.84 | 35 | 0.65 | 14493 | [44] |
| Corn stover | 46.8 | 5.74 | 41.4 | 0.66 | 18101 | [45] |
| Corn stover | 49.4 | 5.6 | 42.5 | 0.6 | 13344 | [46] |
| Corn stover | 43.4 | 6.17 | 45.8 | 1.02 | 17359 | [42] |
| Minimum HHV – kernels | | | | | 15960 | |
| Maximum HHV – kernels | | | | | 17690 | |
| Likeliest Value HHV – kernels | | | | | 17250 | |
| Minimum HHV – stover | | | | | 13340 | |
| Maximum HHV – stover | | | | | 18100 | |
| Likeliest Value HHV – stover | | | | | 15930 | |
| Rape seed | 51.1 | 6.4 | 34 | 2.3 | 21604 | [47] |
| Rape seed | 48.1 | 5.9 | 45.2 | 0.8 | 19330 | [48] |
| Rape seed | 50.5 | 6.3 | 41.2 | 2.1 | 21547 | [49] |
| Rape seed | 50.2 | 6.9 | 37.9 | 5.1 | 22000 | [50] |
| Rape straw | 37.8 | 4.6 | 56.8 | 0.8 | 19380 | [51] |
| Rape straw | 33.7 | 3.9 | 61.8 | 0.7 | 19740 | [47] |
| Rape straw | 44.6 | 5.1 | 48.8 | 1.4 | 17610 | [50] |
| Rape straw | 42.8 | 5.3 | 47.4 | 0.6 | 15788 | [52] |
| Minimum HHV – seed | | | | | 19330 | |
| Maximum HHV – seed | | | | | 22000 | |
| Likeliest Value HHV – seed | | | | | 21575 | |
| Minimum HHV – straw | | | | | 15788 | |
| Maximum HHV – straw | | | | | 19740 | |
| Likeliest Value HHV – straw | | | | | 18495 | |

*Indicates estimate based on Eq. S9

### 1.7 Corn versus corn kernel and canola versus canola seed

In conventional agriculture, corn is generally cultivated for kernels and canola is generally cultivated for seed. The rest of the plant (i.e. stover or straw) may be left in the field or harvested and ground up for use as animal feed (e.g. corn silage). For this study, we wished to utilize the heat content of the entire plant, consistent with the assumption that the most straightforward way to make energy from biomass may be combustion to yield bioelectricity. It was thus desirable to account for the maximum amount of biomass-derived heat that could be grown per unit area, so we computed the composite HHV values summarized in Table S10. Still, it was also necessary to account for the "free" biomass generated as stoveror straw when either corn or canola are grown for the express purpose of producing bioenergy. In particular, it was necessary to adjust literature values for life cycle impacts (e.g. energy use) associated with the production of some unit mass corn kernel or canola. Thus, we assumed that a canola plant and corn plant comprise 33% w/w as seed [22] or 50% w/w as kernel [34] and then divided by the weight fraction comprising seed or kernel to compute life cycle burdens per unit mass whole plant.

## 2 Impact Factor Definitions

### 2.1 Land Use

Land use represents all the land, direct and indirect that would be required to produce the functional unit of energy. This value is influenced by the productivity of the given crop and the HHV of the biomass source. Indirect land use (i.e. "upstream" land use) is associated with the use of industrial chemicals that require land for production. Land use is expressed as hectares (ha).

### 2.2 Water Use

Water use includes direct water usage required to fill algae ponds and irrigate crops. Water use is expressed as $m^3$ of fresh water at the surface. Direct use water streams coming into the systems include precipitation and pumping from surface water reservoirs. Outflows from the agricultural operations include evaporation (algae) and evapotranspiration (corn, canola, and switchgrass) as well as carry-out in the algae biomass. Carry-out includes all the water in the biomass matrix carried with the algae when it is extracted. Indirect water use was included based on the consumption of fertilizers and other inputs, which require water for their production.

### 2.3 Energy Use

Energy use represents the total energy consumption associated with the production of one functional unit of energy. Naturally, the higher the energy use value, the lower the efficiency of the bioenergy source. The functional unit was not included in eacg reported energy use number since it is the same for each crop inherent to the definition of a functional unit. Thus, the total energy use number reported here includes the energy required for cultivation and preliminary transportation of each crop. Indirect energy associated with production of input chemicals is also included. Energy is reported here in terms of megajoules (MJ).

### 2.4 Global Warming Potential

Global warming potential was quantified in terms of kilogram equivalents of $CO_2$ using the global warming potential values adopted by the Intergovernmental Panel on Climate Change (IPCC) [53]. The values for a 100 year time horizon were selected and are summarized in Table S11. $CO_2$ sequestered in the biomass was subtracted from the total greenhouse gas emissions for the agricultural process.

**Table S11.** Global warming potential (GWP) values used to estimate total impacts reported in this study.

| Gas | GWP (100 year time horizon) |
|---|---|
| Carbon Dioxide | 1 |
| Methane | 25 |
| Nitrous Oxide | 298 |

### 2.5 Eutrophication

Eutrophication was expressed in terms of $PO_4^{3-}$ mass equivalents. Conversion factors for the four compounds included in this composite impact category are provided in Table S12. As with the other impact factors, both direct and indirect contributions were included. Direct contributions were estimated based on a stochastic rate of fugitive emissions (spills) that could be reasonably expected in an algae production facility. Indirect contributions (i.e. "upstream" contributions) arise during upstream processes such as fertilizer production, electricity generation and transmission, etc.

**Table S12.** Eutrophication potential values used to estimate the total potential reported in this study.

| Pollutant Type | Eutrophication Equivalence (g $PO_4^-$eq/g substance) |
|---|---|
| COD | 0.022 |
| Nitrogen | 0.42 |
| Nitrate | 0.1 |
| Phosphorus | 3.06 |

## 3 Impact Factor Calculations

The impacts associated with algae cultivation are described in detail below. The impacts for canola, corn, and switchgrass were used as reported in the Ecoinvent database and referenced against other published data. Since these are published values, they are not discussed in detail here.

### 3.1 Land Use

Land use is reported in hectares (ha) because this is the SI unit of area (1 ha = 10,000 $m^2$ = 2.47 acre). It was assumed that not all land dedicated toward the production of a biofuel is used for direct cultivation. Access roads, buildings, and other infrastructure are needed. For corn, canola, and switchgrass these contributions were included in the Ecoinvent data. For algae, a 25% increase in land area was included to account for the footprint of support infrastructure.

### 3.2 Water Use

Water use was computed using the precipitation and evaporation data presented in Section 1. Overall, indirect contributions from the production of chemicals used in algae cultivation were much greater than the direct use contributions. This is demonstrated in the paper.

### 3.3 Energy Use

Energy use includes all the energy inputs that would be required to produce one functional unit. This measure captures the primary energy needed for all the material inputs to the process (e.g., fertilizers) as well as the energy needed to run the farming operation (e.g., mixing, centrifuges). Since energy demands of these processes are driven entirely by movement of water through the ponds, a harvesting model was created to estimate flows as a function of pond productivity. This water and algae balance was performed to determine: 1) The volume of algae solution to be separated as a function of productivity (harvesting rate); and 2) the flow of make-up water required to maintain a constant pond volume as a function of productivity and evaporation (make-up rate). This balance, presented in Figure S4, shows that the volume entering the centrifuge ($Q_2$) is the product of the pond's productivity and the pond area (in L/day). The concentration (factor of 1000x) cancels in the unit conversion between g → kg → L algae solution. The make-up rate depends very much on evaporation rate and carry out rate ($Q_1$).

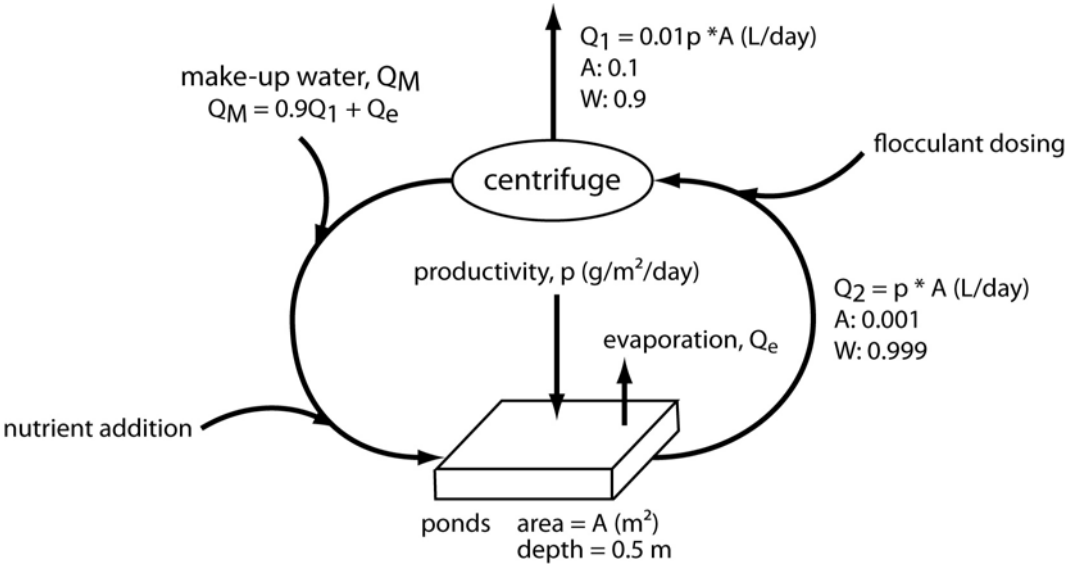


**Figure S4.** Schematic of algae and water flows through the ponds. The equations presented here were used to estimate water and algae flows as a function of pond productivity. These flows were in turn used to estimate the energy demands during algae cultivation.

Demonstration scale studies of algae production have found that energy demands can be divided into several classes: mixing (24.4%); harvesting/processing (17.4%); water supply (19.8%); flue gas supply (34.8%); and other (3.5%) [3]. For our model, it was assumed that $CO_2$ can be delivered as a pure gas such that flue gas supply was not required. As such, our estimates for the other energy streams were divided up roughly as follows: mixing (25.5%); harvesting (43.7%); and water supply (30.8%). This breakdown is approximately proportional to Benemann's allocation [3], and differences could be easily attributed to differences in pond architecture or machinery efficiency.

#### *3.3.1 Mixing*

The energy required to operate a paddle wheel depends on its size and rotation speed. The energy required by one paddle wheel was modeled using a triangular distribution over the range 0.0001 kW to 0.01 kW (likeliest value = 0.037 kW) [54]. We assumed 10 paddle wheels were used per hectare (roughly a density of 1 paddle wheel per 100 $m^2$ of ponds) operating at ~10 RPM. This constitutes an energy demand of approximately 0.01 W as shown in Eq. S10.

$$P = 0.037\ kW/paddle\ wheel \times 10\ paddle\ wheels/ha \times 3.15 \times 10^{7}\ s/yr = 11{,}668\ MJ/ha\ yr \quad \text{Eq. S10}$$

*3.3.2 Centrifugation*

We assumed that a combined flocculation/centrifugation process is used to separate the solids from the medium. Alum was utilized as the flocculent, and dosing was consistent with previous reports by Becker [55]. Algae concentrations entering and exiting the centrifuge were assumed to be 0.1% mass per volume (m/v) and 10%, respectively. We assumed the centrifuge to be of the sediment-type configuration. The energy for such a unit can be approximated as the sum of the energy to accelerate the feed stream and the power to discharge the solid cake, $P_{total} = P_{acc} + P_{con}$, where $P_{acc}$ is the power to accelerate feed stream from zero speed to full tangential speed at the pool required to achieve sufficient G-force for separation. This is expressed in Eq. S11.

$$P_{acc} = 5.984 \times 10^{-10} \times sg \times Q \times (\Omega r_p)^2 \quad \text{Eq. S11}$$

Here *sg* is the specific gravity of the mixture (1 kg/L), *Q* is the flow rate of mixture (in gal/min), *Ω* is the rotational speed of centrifuge ($min^{-1}$), and $r_p$ = radius of centrifuge bowl (m).

$P_{con}$ is the power to convey and discharge cake and it can be calculated using the relationship in Eq. S12.

$$P_{con} = 1.587 \times 10^{-5} \times D \times T \quad \text{Eq. S12}$$

Where $\Delta$ is the differential speed and it can be calculated using Eq. S13:

$$\Delta = \sqrt{\left(\frac{k_1}{k_2}\right)^2 + \frac{1}{k_2} \times m_{ss} \times I \times G \times L_{eff}} - \frac{k_1}{2k_2} \quad \text{Eq. S13}$$

Here, $k_1$ was assumed to be 80 bar, $k_2$ is 5.3 bar, $g_c$ is 32.2 lbf-ft/lbm-$s^2$, *I* is 0.5, $m_{ss}$ is the dry feed rate basis (10 kg/sec), *G* is 770 g, the length to diameter ratio (L/D) is 3, the diameter of the bowl (*D*) is 690 mm, L is 2070 mm, and the effective length $L_{eff}$ is (2/3)L so 1380 mm (54.33 in). The conveyance torque (*T*) is $T = k_1 + k_2 \times \Delta$. This torque value is then plugged back into equation S11 and the $P_{con}$ and $P_{acc}$ values are added together to get the power requirements on the centrifuge. The energy estimates obtained here correspond well with published values for centrifuges with comparable specifications [56].

*3.3.3 Water supply*

Energy is required to pump water into and among the ponds as well as to the centrifuges. This energy requirement was estimated by calculating the head through the pump using Eq. S14.

$$h = \frac{P_2 - P_1}{\rho g} \quad \text{Eq. S14}$$

Here $P_2$ and $P_1$ are the pressure at the pump inlet and outlet, respectively. Inlet pressure was assumed to be 0.1 MPa, and outlet pressure was assumed to be 0.2 MPa. g is the acceleration of gravity, and $\rho$ is the density of water. Work in the pump is then estimated, using h as derived from Eq. S14, via Eq. S15:.

$$W = \frac{hg}{\eta} \quad \text{Eq. S15}$$

Where $W$ is the work in J/s, $g$ is the acceleration of gravity, and $\eta$ is the pump efficiency (85%).

*3.3.4 Infrastructure Manufacturing*

The life cycle impacts associated with manufacture and installation of the pumps, paddle wheels, and centrifuge were estimated using SimaPro and ultimately found to be negligible relative to the magnitude of the impacts associated with other life cycle stages. The total energy draw of the overall system during operation (included in the model) was on the order of 1.1 kW/ha. This value was used to size the physical components needed to operate the ponds. Based on data from the SimaPro database, the impacts associated with building these unit operations was less than 1% of the total impact for one year (land use = 8.3E-4 ha, water use = 847 $m^3$, energy use = 1870 MJ, GHG = 121 kg $CO_2$e, 7E-3 kg $PO_4$e). Over the life of a pond, e.g., tens of years, it is reasonable to assume that the 'use phase' energy requirements dominate over the production and manufacture energy requirements.

*3.3.5 Other*

The $CO_2$ was stored as a liquid and delivered as a gas such that no energy was modeled for pH-mediated on-demand delivery of $CO_2$. There will be an energy draw associated with buildings and other infrastructure serving the algae production process. Here we've assumed 3% of the total energy needed to operate the production facility will be required for this purpose, consistent with Benemann [57].

### 3.4 Global Warming Potential

Greenhouse gas (GHG) emissions from the production of algae were calculated by adding the emissions associated with all the inputs to the process (e.g., fertilizer, energy, etc) and subtracting out the rate at which algae take up $CO_2$ when they grow. This rate was estimated based on the stoichiometry of an algal cell and was made stochastic based on the fact that algae bind carbon in biomolecules that are later excreted as algal organic mass. This carbon content is not included in the total biomass produced since it cannot be centrifuged from solution given its dissolved state. Based on stoichiometry, 91 moles of $CO_2$ is consumed for every mole of algae produced. Multiplying through by the molecular weight of each material, the expected sequestration rate is 1.7 g $CO_2$/g algae. Four additional empirical measurements for this ratio, ranging from 0.99 – 1.96 were taken from the literature [28, 29, 58]. These five values were then fit to a normal distribution with average ($\mu$) = 1.6 g $CO_2$/g algae and standard deviation ($\sigma$) = 0.3 g $CO_2$/g algae. The Anderson-Darling statistic for this fit was 0.99, indicating a reasonable fit for this data.

### 3.5 Eutrophication

Eutrophication impacts for the production of algae included contributions from each of the inputs to the process (e.g., fertilizer) and also assumed a small amount of fugitive losses asa function of the amount of algae produced. A uniform distribution was used to model these losses over the range reported in the literature, 1E-6 – 1E-5 kg $PO_4$-eq per kg dry yield algae [3]. For a well managed outdoor pond system, these losses are likely to be much lower than nutrient run off from conventional agricultural operations.

## 4 Life Cycle Inventory Data

### 4.1 Canola, Corn, and Switchgrass Production

**Table S13.** Life cycle impacts for canola seed, corn kernel, and grass silage production as taken from the Ecoinvent Database [43]. GHG is greenhouse gas emissions; EUT is eutrophication potential. Impact factors were assigned lognormal distributions using averages ($\mu$) and standard deviations ($\sigma$) from the data source. These parameters are presented for each distribution using $\mu/\sigma$ notation.

| Item | Functional Unit | Impact category | | | | |
|---|---|---|---|---|---|---|
| | | Land Use ($m^2$) | Water Use ($m^3$) | Energy Use (MJ) | GHG ($CO_2$-eq) | EUT ($PO_4$-eq) |
| Canola | 1 kg dry rapeseed | 0.11/0.021 | 1.8/1.78 | 11.9/11.6 | 1.87/1.86 | 5E.1-3/5E-3 |
| Corn | 1 kg dry weight | 0.12/0.012 | 0.06/0.007 | 0.36/0.052 | 0.062/0.004 | 1.4E-6/2E-7 |
| Switchgrass | 1 kg dry weight | 0.84/0.186 | 0.15/0.018 | 1.46/0.152 | 0.220/0.039 | 4.4E-6/8E-7 |

### 4.2 Algae Production

**Table S14.** Life cycle impacts for electricity and chemicals used in algae production [43] as taken from the Ecoinvent Database [43]. GHG is greenhouse gas emissions; EUT is eutrophication potential. Impact factors were assigned lognormal distributions using averages ($\mu$) and standard deviations ($\sigma$) from the data source. These parameters are presented for each distribution using $\mu/\sigma$ notation.

| Item | Functional Unit | Impact category | | | | |
|---|---|---|---|---|---|---|
| | | Land Use ($m^2$) | Water Use ($m^3$) | Energy Use (MJ) | GHG ($CO_2$-eq) | EUT ($PO_4$-eq) |
| Electricity (US mix) | 1 kWh | 0.005/0.006 | 0.76/0.010 | 2.5/2.42 | 0.21/0.010 | 2.2E-6/2E-6 |
| Alum | 1 kg $Al_2(SO_4)_3$ | 0.013/0.008 | 2.51/0.474 | 5.7/1.29 | 0.51/0.073 | 9.0E-4/8E-5 |
| Superphosphate | 1 kg $P_2O_5$ | 0.090/0.050 | 7.16/1.090 | 24.7/3.99 | 2.09/0.205 | 8.4E-5/8E-5 |
| Urea | 1 kg N | 0.062/0.049 | 3.99/1.290 | 62.1/11.8 | 3.37/0.335 | 1.7E-4/2E-4 |
| $CO_2$* | 1 kg $CO_2$ | 0.021/0.028 | 2.16/0.600 | 8.3/1.95 | 0.82/0.137 | 3.6E-5/1E-5 |

* Since $CO_2$ is modeled as a byproduct of ammonia production (whereby methane is split using steam to create hydrogen and $CO_2$), the associated burdens can be allocated between $CO_2$ and $H_2$ production using a 50/50 split. As such, the numbers reported here are twice what was included in the model as burdens associated with $CO_2$ production.

## 5 Synergies with Municipal Wastewater Treatment

### 5.1 Wastewater Effluents

Partially treated municipal wastewater effluents were evaluated for their utility as nutrient sources during large scale algae cultivation. Three different effluents were assessed: (1) secondary effluent from an activated sludge treatment plant with biological nutrient removal for N and P (BNR); (2) secondary efflu-

ent from a conventional activated sludge treatment plant with nitrification (CAS); and, (3) a 3.5% solution of hydrolyzed urine from a source-separated collection system (SSU). This volume of urine is the amount produced by roughly 900 people per year [59]. Table S15 summarizes nutrient concentrations for each of these wastewaters and the sources from which this data were taken. Though direct dosing of ammonia is known to inhibit algae growth, it was assumed that urine ammonia is rapidly hydrolyzed to ammonium such that use of the urine has no deleterious effect on algae growth, as demonstrated by Kim et al (2007) [60].

**Table S15.** Three types of wastewater effluents evaluated in this investigation and their respective concentrations of total nitrogen (N) and total phosphorus (P).

| Wastewater | Total N (mg/L) | Total P (mg/L) | Source |
|---|---|---|---|
| BNR | 3 – 8 | 1 – 2 | [61] |
| CAS | 15 – 35 | 4 – 10 | [61] |
| SSU | 4100 – 4600 | 200 - 220 | [62] |

For each of these wastewaters, distributions of total N and total P were assumed to be uniform over the ranges indicated in Table S15. For the case of CAS and BNR, it was assumed that use of partially-treated wastewaters would completely supplant the need for freshwater into the algae cultivation ponds. Even so, additional chemical fertilizers would be required to meet the N and P requirements. In contrast, a 3.5% solution of hydrolyzed urine in water was found to contain an amount of nitrogen almost exactly equivalent, on average, to the algae's N demand. To avoid introducing more N than could be directly taken up by the algae, the concentration of the source-separated urine was capped at a 3.5%. It was assumed that additional superphosphate would be added to meet the full P demand. A 3.5% solution strength is consistent with previous experiments in which a 3% solution of fermented swine urine was used for bench-scale algae culture [60].

### 5.2 Modeling Burden Offsets

It was expected that three types of burden reductions would be associated with use of wastewater treatment effluents as nutrient sources during large-scale algae cultivation. These included: 1) offsets associated with reduced need for fertilizer production; 2) offsets associated with reduced need for wastewater treatment (WWT) and its associated material and energy inputs; and 3) offsets in freshwater usage since the wastewater effluent is utilized as algae growth medium. Computation of these offsets is summarized in the following paragraphs.

#### *5.2.1 Offset Fertilizer Production Burdens*

For computation of the burden offset associated with reduced fertilizer production in each wastewater scenario, total N and P requirements were first computed on the basis of nutrient demand. This computation is outlined in §1.5. These quantities were then multiplied by their respective life cycle impact factors from Ecoinvent® to estimate reductions in each impact area associated with decreased fertilizer usage. Life cycle inventory data for urea and superphosphate, the chemical fertilizers partially supplanted by use of wastewater nutrients, are summarized in Table S14 (§4.2).

#### *5.2.2 Offset Wastewater Treatment Burdens*

It was expected that each of the partially-treated wastewaters, if not used as nutrient sources for algae cultivation, would otherwise have to undergo nutrient removal in a municipal wastewater treatment plant (WWTP). The WWTP's fully-treated effluents would then be subject to stringent nutrient standards under Virginia's Pollution Discharge Elimination System (VPDES) Tier 4 Effluent Guidelines [63]. For this reason, the burdens that would have been accrued during WWT were counted as negative burdens (i.e.

offsets) for the algae life cycle. Final effluent concentrations of total N and total P were assumed to 3.0 be mg/L and 0.1 mg/L, respectively.

Life cycle impact data for removal of 1 kg nitrogen was taken from Maurer et al (2003) [64]. N removal was assumed to proceed via nitrification and subsequent denitrification with addition of methanol as external carbon source. A ratio of 3.4 kg methanol per 1 kg N eliminated [65] was used to compute the mass of methanol required to reduce each wastewater's initial nitrogen concentration down to the VPDES acceptable limit (3.0 mg/L). This quantity of methanol was then multiplied by Ecoinvent® impact factors for methanol production (e.g., 37.5 MJ per 1 kg methanol). Electricity consumption for aeration during nitrification was also assessed, using a value of 10 MJ per 1 kg N eliminated.

Life cycle impact data for removal of 1 kg phosphorus was also taken from Maurer et al (2003) [64]. P removal was assumed to proceed via chemical precipitation with ferrous sulfate. A ratio of 1.8 kg Fe per 1 kg P removed was used to compute the amount of ferrous sulfate required to reduce each wastewater's initial phosphorus concentration down to the VPDES acceptable limit (0.1 mg/L). This quantity was then multiplied by Ecoinvent® impact factors for iron (II) sulfate production (e.g., 1.95 MJ per 1 kg $Fe(II)SO_4$). Energy consumption for transportation of the resulting precipitant sludge was estimated to be 2 MJ per kg P eliminated.

### *5.2.3 Offset Freshwater Burdens*

It was assumed that effluent used to deliver nutrients as fertilizer offset could also serve as algae growth medium. Thus, for the BNR and CAS cases, the direct freshwater requirements could be completely eliminated. In contrast, it was assumed that the source-separated urine would need to be diluted to a 3.5% solution in freshwater to satisfy the algae's nitrogen demand without compromising algal growth. Thus the SSU scenario reflects only a 3.5% offset in direct water use relative to the VA base case scenario direct water usage.

## 5.3 Wastewater Treatment Life Cycle Inventory Data

Impact factors for fertilizer avoidance, as mediated by use of wastewaters as N and P source, are summarized in Table S14 in §4.2. Additional life cycle data for chemicals utilized in the removal of nutrients from municipal wastewater are summarized in Table S16.

**Table S16.** Life cycle impacts for electricity and chemicals used to model offset life cycle burdens associated with avoidance of wastewater treatment [43]. GHG is greenhouse gas emissions; EUT is eutrophication potential. Impact factors were assigned lognormal distributions using averages ($\mu$) and standard deviations ($\sigma$) from the Ecoinvent Database. These parameters are presented for each distribution using $\mu/\sigma$ notation.

| Item | Functional Unit | Impact category | | | | |
|---|---|---|---|---|---|---|
| | | Land Use ($m^2$) | Water Use ($m^3$) | Energy Use (MJ) | GHG ($CO_2$-eq) | EUT ($PO_4$-eq) |
| Electricity (US mix) | 1 kWh | 0.005/0.006 | 0.76/0.010 | 2.5/2.42 | 0.21/0.010 | 2.2E-6/2E-6 |
| Ferrous sulfate | 1 kg $Fe(II)SO_4$ | 0.017/0.015 | 1.30/0.416 | 2.0/0.97 | 0.19/0.066 | 8.3E-6/7E-6 |
| Methanol | 1 kg $CH_3OH$ | 0.007/0.002 | 4.30/0.122 | 37.5/5.35 | 1.67/0.073 | 4.2E-5/4E-6 |

## 6 Additional Results

### 6.1 Tornado Plots

Tornado plots for eutrophication potential, net water use, and land use corresponding to production of one functional unit from algae show how sensitive these parameters are to each model input. This information is summarized in Figure S5. A scan was performed to identify the five inputs for which wach impact factor is most sensitive. In the case of land use, only three are reported because the impact of other model inputs is very small. For each case, the centerline represents the baseline case. The dark and light shaded values indicate direct and inverse relationships respectively. In each case, the importance of algae high heating value is apparent but the influence of nutrient (Urea and $CO_2$) is also evident for eutrophication and water use. This is because of the life cycle burdens associated with production of these nutrients. For land use, total irradiation and radiation use efficiency (RUE) are found to be important drivers of overall algae burdens.

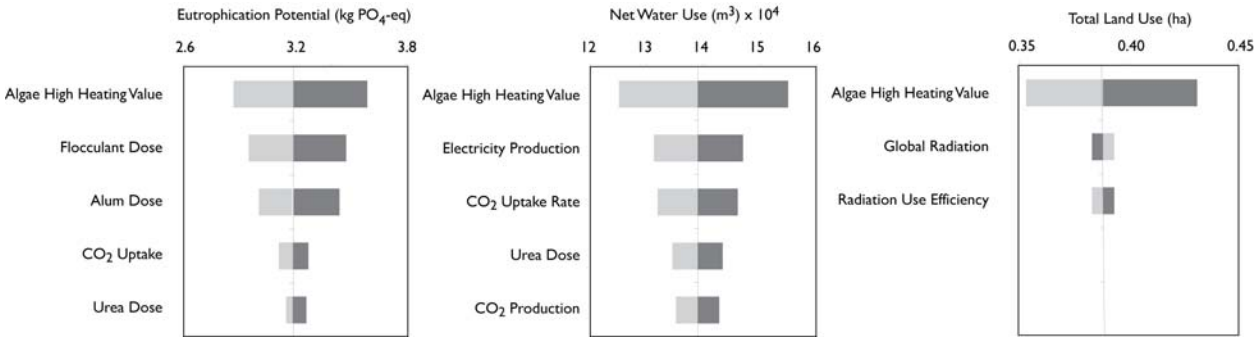


**Figure S5.** Tornado plots for the three impact factors not presented in manuscript. Tornado plots reveal the extent to which these environmentally burdens associated with algae cultivation are sensitive to a ±10% change in each of several input parameters.

### 6.2 Results Distributions

Table S18 summarizes best-fit distributions for life cycle impact outputs from the various crops model in each selected geographic location (VA = Roanoke, Virginia, USA; IA = Ames, Iowa, USA; CA = San Diego, California, USA). This same table also presents 95% confidence intervals for the mean values of each parameter presented in Table 1 of the main text document.

**Table S18** Best-fit distributions and 95% confidence intervals for life cycle impacts associated with production of one functional unit from algae, canola, corn, or switchgrass in three geographic locations.

| Impact Category | Location | Best-Fit Distribution | Algae 95% CI | Canola 95% CI | Corn 95% CI | Switchgrass 95% CI |
|---|---|---|---|---|---|---|
| Land Use (ha) | VA | Gamma | [0.3,0.5] | [1.7,2.5] | [0.9,2.1] | [1.0, 2.9] |
| | CA | Gamma | [0.3, 0.5] | [2.0,3.0] | [0.8,1.9] | [0.5, 1.5] |
| | IA | Gamma | [0.5, 1.1] | [1.8, 2.7] | [0.9,2.1] | [1.0, 2.9] |
| Energy Use (MJ) | VA | Gamma | [190000,450000] | [55300,88000] | [31900,45700] | [25000, 35700] |
| | CA | Gamma | [251000, 556000] | [55300,87800] | [36200,40900] | [25000, 35900] |
| | IA | Gamma | [224000, 546700] | [55400, 88300] | [36100,40900] | [24900, 36000] |
| Water Use (m3) | VA | Gamma | [76000,170000][a] | [7930,13500] | [4100,12000] | [1400, 9800][a] |
| | CA | Gamma | [101000, 216000] | [9700,15000] | [9800,17000] | [6700, 14500] |
| | IA | Gamma | [95900, 219000] | [8600, 14200] | [8300,15000] | [5200, 13000] |
| Greenhouse Gas Emissions (kg $CO_2$-eq) | VA | Beta | [7641,30540] | [-18200,-14100] | [-28000,-24000] | [-27800, -20900] |
| | CA | Beta | [12400, 36500] | [-18100,-14000] | [-28000,-25000] | [-27700, -20900] |
| | IA | Beta | [8900, 36000] | [-18200, -14100] | [-28000,-25000] | [-27800, -20900] |
| Eutrophication Potential (kg $PO_4$-eq) | VA | Lognormal | [1.99,5.42] | [18.6,41.4] | [17.2,38.0] | [3.4, 10.4] |
| | CA | Lognormal | [2.1, 5.5] | [18.5,41.4] | [16.8,38.5] | [3.4, 10.3] |
| | IA | Lognormal | [2.0, 5.4] | [18.5, 41.3] | [17.0,39.0] | [3.4, 10.4] |

[a] Slightly better fit using logistic distribution.
[b] Slightly better fit using lognormal distribution.

As evident in Table S18, best-fit distributions for each type of life cycle impact tended to be consistent among the three geographic locations. As such, sample histograms are presented for outputs from the Virginia model only. These are depicted in Figures S6 – S9. In each figure, the green line represents the best-fit statistical distribution referenced in Table S18. The blue portion of each figure corresponds to the 95% confidence interval, and the red portions correspond to area in the two tails ($\alpha/2 = 0.025$).

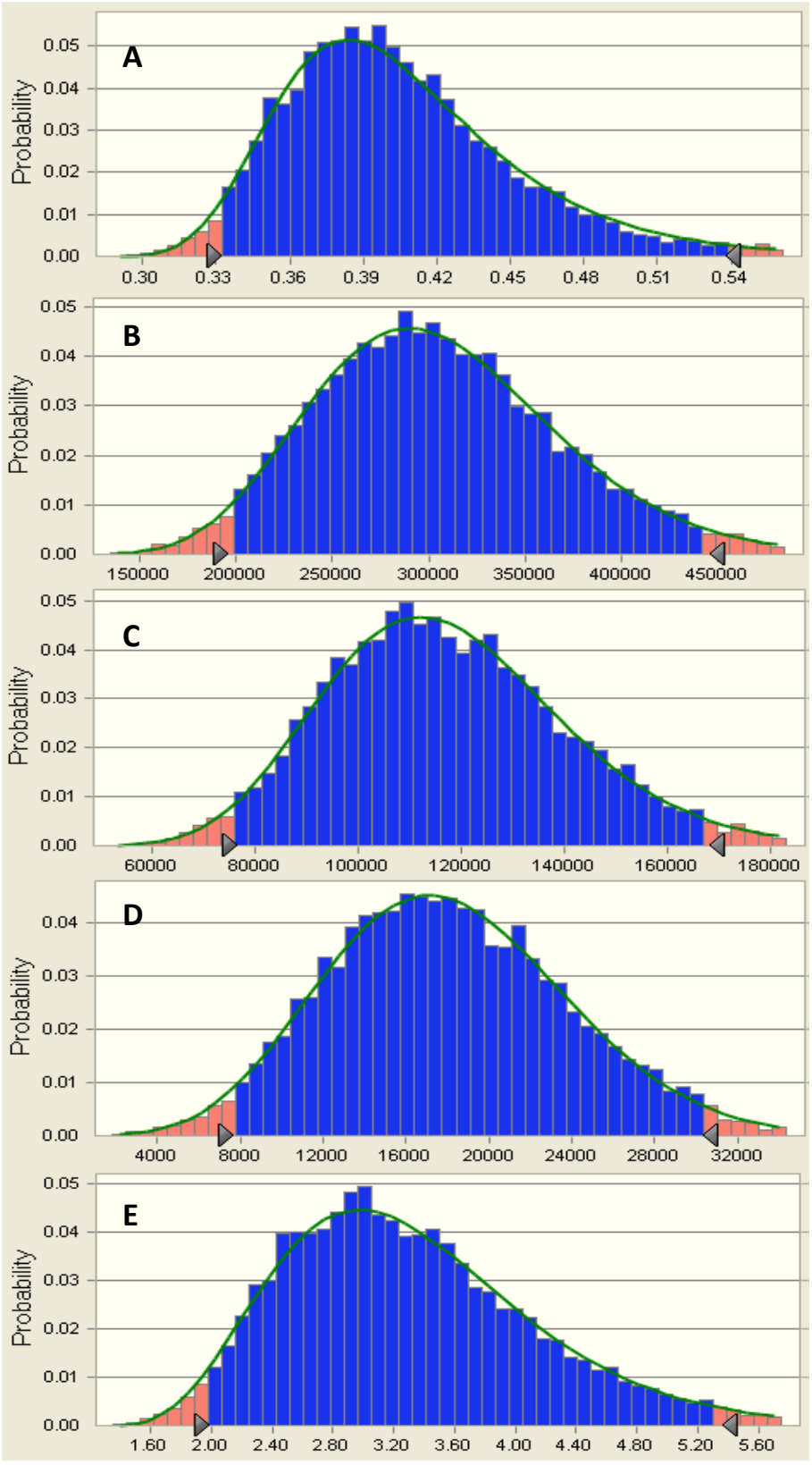


**Figure S6.** Output distributions for land use (A), energy use (B), water use (C), greenhouse gas emissions (D), and eutrophication potential (E) for production of one functional unit from algae in VA.

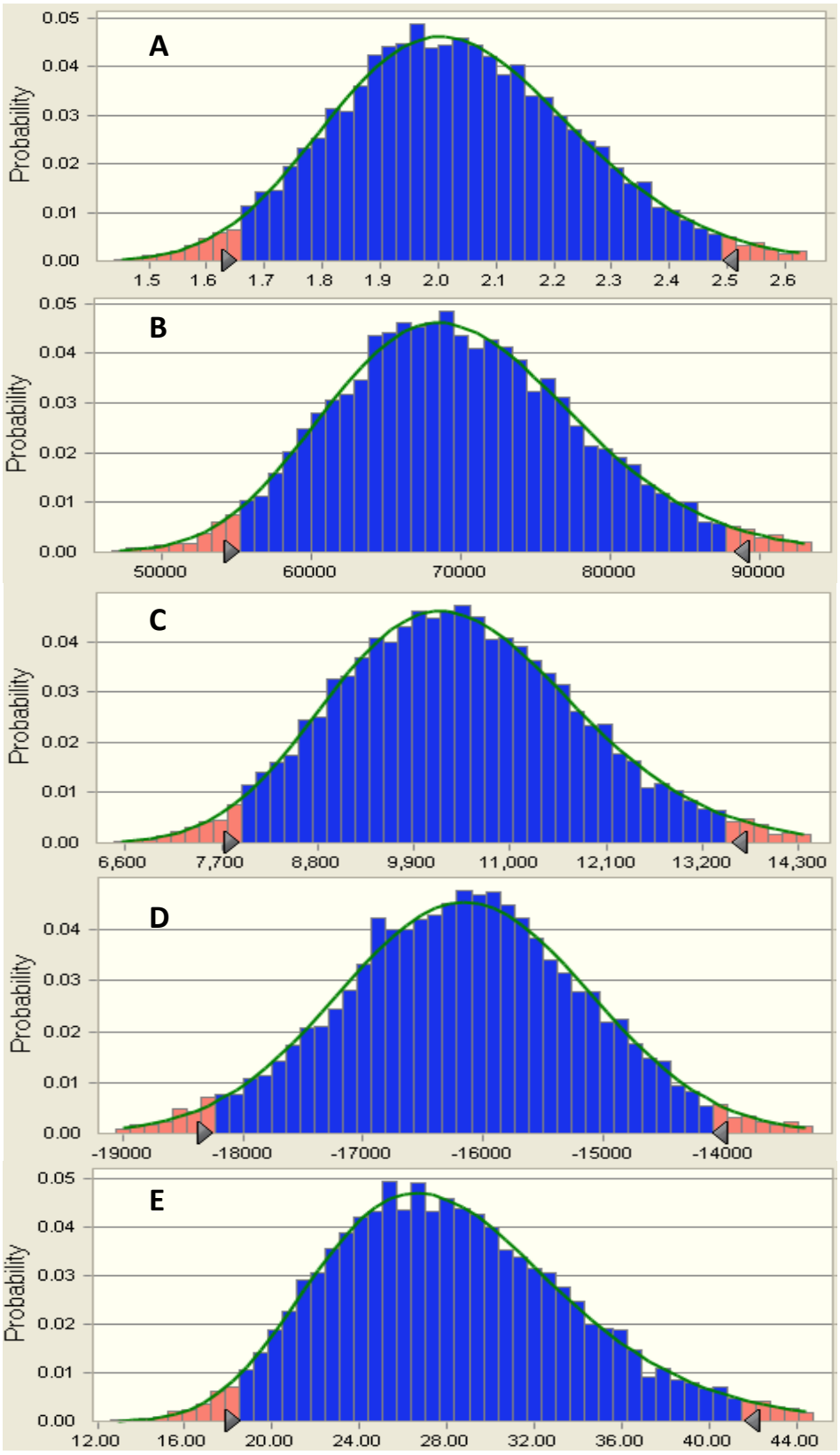


**Figure S7**. Output distributions for land use (A), energy use (B), water use (C), greenhouse gas emissions (D), and eutrophication potential (E) for production of one functional unit from canola in VA.

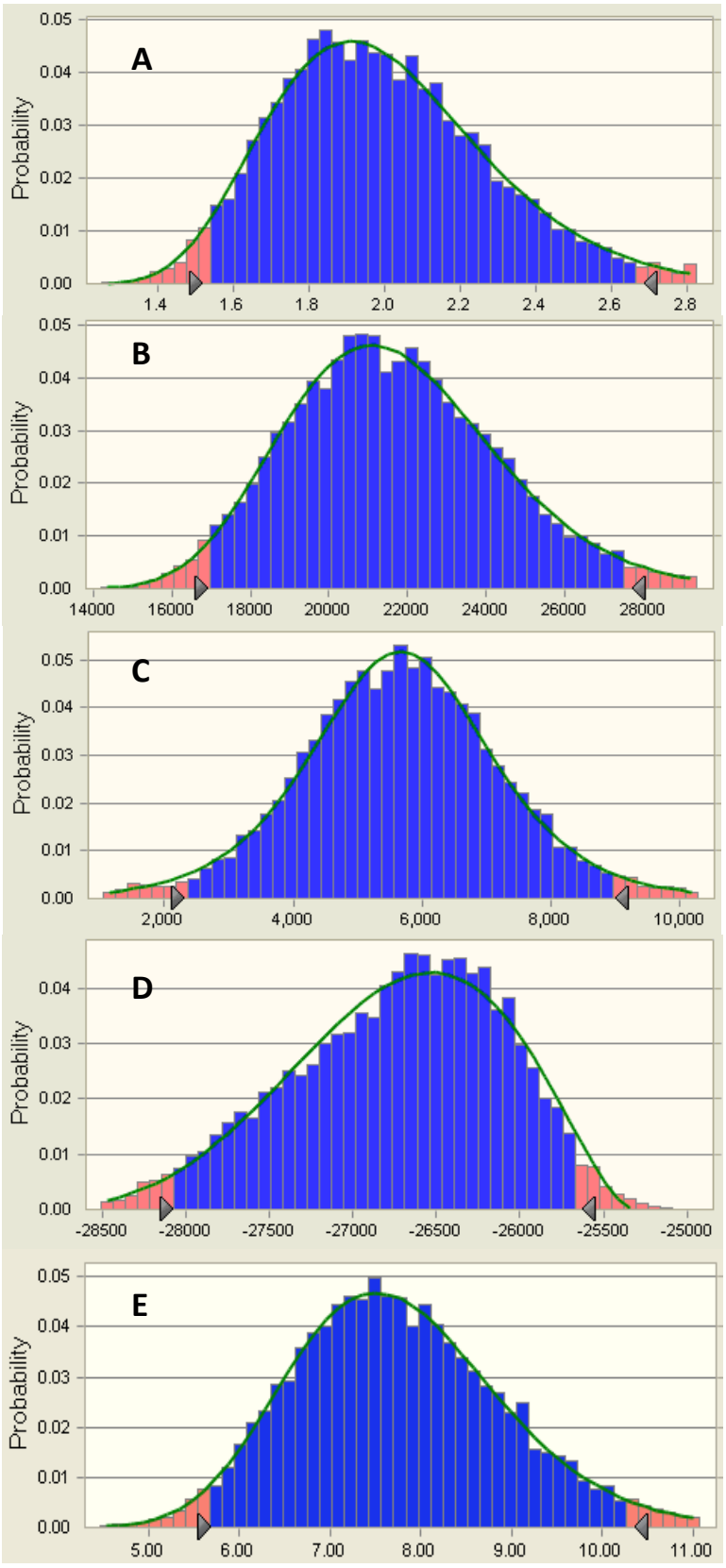


**Figure S8.** Output distributions for land use (A), energy use (B), water use (C), greenhouse gas emissions (D), and eutrophication potential (E) for production of one functional unit from corn in VA.

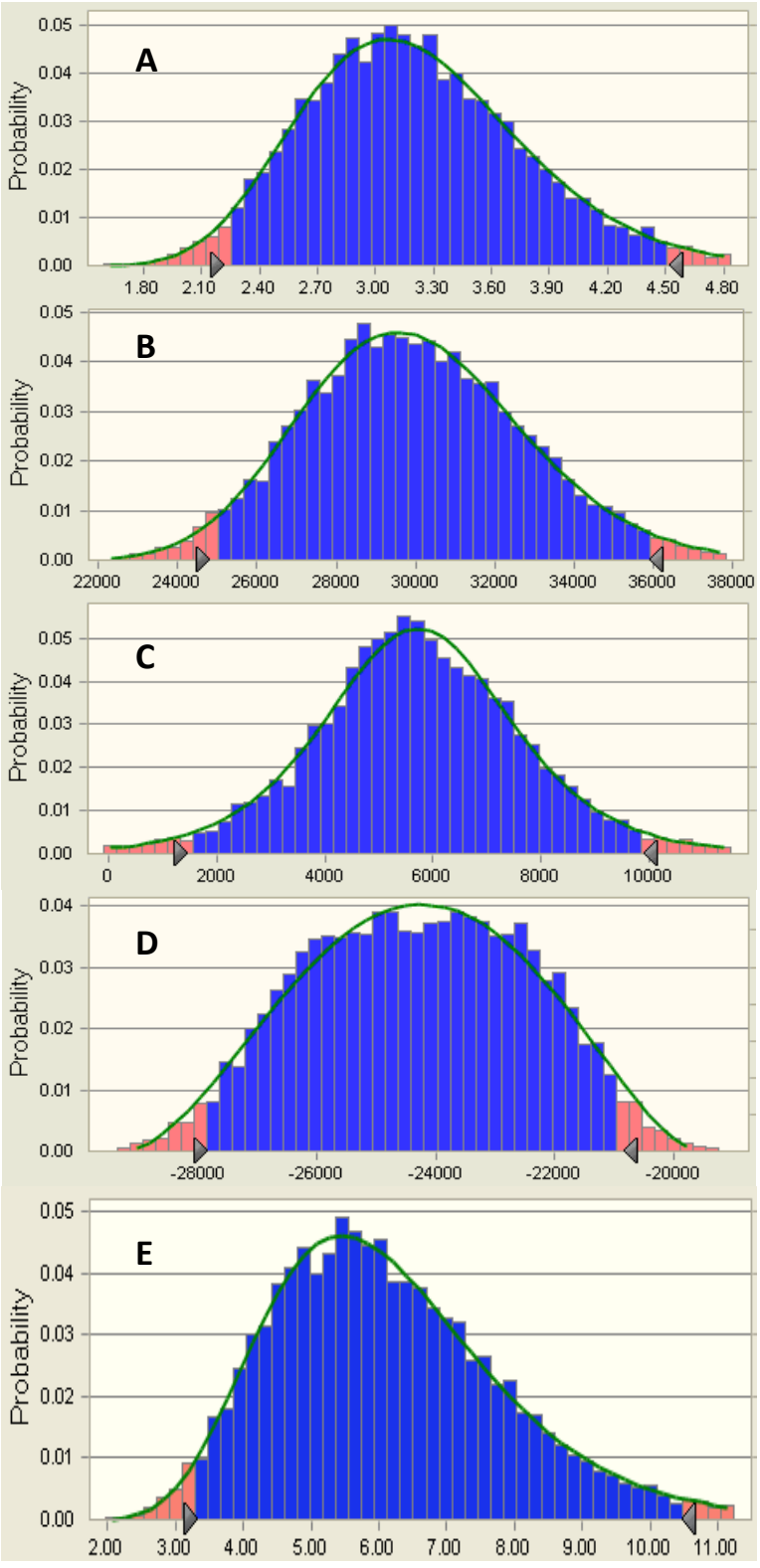


**Figure S9.** Output distributions for land use (A), energy use (B), water use (C), greenhouse gas emissions (D), and eutrophication potential (E) for production of one functional unit from switchgrass in VA.

**References**


1. EIA, *Energy Information Administration*. 2008.
2. NREL, National Solar Radiation Database (1961-1990). . In National Renewable Energy Laboratory 1994.
3. Benemann, J.; Oswald, W. *Systems and Economic Analysis of Microalgae Ponds for Conversion of CO2 to Biomass - Final Report*; Department of Energy: Pittsburgh, 1996; p 201.
4. NOAA, Surface Radiation Network (SURFRAD). In National Oceanic and Atmospheric Administration: 2009.
5. Perry, R. H.; Green, D. W., *Perry's Chemical Engineers' Handbook*. 7th Edition ed.; McGraw-Hill: 1997.
6. Howell, T.; Evett, S., The Penman-Monteith Method, Section 3. In *Evapotranspiration: Determination of consumptive use in water rights*, Denver, CO, 2004.
7. ASCE, The ASCE Standardized Reference Evapotranspiration Equation. In American Society of Civil Engineers: 2002.
8. USNO, Astronomical Applications: Complete sun and moon data for one year. In Observatory, U. N., Ed. 2009.
9. Brann, D.; Abaye, A.; Peterson, P., *Virginia Agronomy Handbook*. Virginia Polytechnic Institute and State University: Blacksburg, VA., 2009.
10. Kiniry, J.; Jones, C.; O'Toole, J.; Blanche, R.; Cabelguenne, M.; Spanel, D., Radiation-use efficiency in biomass accumulation prior to grain-filling for five grain-crop species. . *Crop Research* **1989,** *20*, 51-64.
11. Maddonni, M.; Otegui, M., Leaf area, light interception, and crop development in maize. *Field Crop Research* **1996,** *48*, 81-87.
12. USDA, California Corn for Silage Acreage, Yield, and Production by County. In NASS, C. F. O. S., CA., Ed. US Department of Agriculture 2006.
13. Thoreson, D.; Lang, B. *2008 Corn Silage Yield Trial*; Ames, IA., 2009.
14. Adler, P.; Sanderson, M.; Boateng, A.; Weimer, P.; Jung, H., Biomass yield and biofuel quality of switchgrass harvested in fall or spring. *Agronomy Journal* **2006,** *98*, 1518-1525.
15. Lemus, R. Switchgrass as an energy crop: Fertilization, cultivar, and cutting management. Virginia Polytechnic Institute and State University, Blacksburg, VA. , 2004.
16. Adler, P. R.; Sanderson, M. A.; Boateng, A. A.; Weimer, P. J.; Jung, H.-J. G., Biomass Yield and Biofuel: Quality of Switchgrass Harvested in Fall or Spring. *Agron J* **2006,** *98*, (6), 1518-1525.
17. Putnam, D., Switchgrass and alfalfa as cellulosic biofuels: Possibilities and limitations. In *Proceedings of the 2008 California Alfalfa and Forage Symposium and Western Seed Conference*, San Diego, CA., 2008.
18. Gibson, L.; Bernhart, S., *Switchgrass (AG 200)*. Ames, IA, 2007.
19. Hang, A. N.; Collins, H. P.; Sowers, K. E. *Irrigated spring and winter canola production in Washington*; University of Washington Extension: Pullman, WA, 2009; p 7.
20. Parsons, C. E. *Canola Yield Data*; University of Arkansas Division of Agriculture: 2006.
21. NREL, National Solar Radiation Database Update (1991-2005). . In National Renewable Energy Laboratory 2005.
22. Thomas, P., Chapter 3: Growth Stages. . In *Canola Council of Canada's Canola Growers Manual*, 2003.
23. Rife, C. *National winter canola variety trial*; Kansas State University Agricultural Experiment Station and Cooperative Extension Service: Manhattan, KS., 2003.
24. Starner, D.; Bhardwaj, H.; Hamama, A.; Rangappa, M., Canola production in Virginia. In *Progress in new crops*, Janick, J., Ed. ASHS Press: Alexandria, VA., 1996; pp 287-290.

25. Bañuelos, G., Irrigation of broccoli and canola with Boron- and Selenium-laden effluent. *Journal of Environmental Quality* **2002,** *31*, 1802-1808.
26. Schill, S., Canola waits in the wings. *Biodiesel Magazine* 2008.
27. Kadam, K. L., Environmental benefits on a life cycle basis of using bagasse-derived ethanol as a gasoline oxygenate in India. *Energy Policy* **2002,** *30*, (5), 371-384.
28. Weissman, J. C.; Tillett, D. M. *Design and Operation of an Outdoor Microalgae test Facility: Large-Scale System Results*; NREP: Golden, CO, 1990.
29. Kadam, K. L., Environmental implications of power generation via coal-microalgae cofiring. *Energy* **2002,** *27*, (10), 905-22.
30. Chisti, Y., Biodiesel from microalgae. *Biotechnology Advances* **2007,** *25*, (3), 294-306.
31. Del Campo, J.; García-González, M.; Guerrero, M., Outdoor cultivation of microalgae for carotenoid production: current state and perspectives. *Applied Microbiology and Biotechnology* **2007,** *74*, (6), 1163-1174.
32. Redfield, A. C., The biological control of chemical factors in the environment. . *American Scientist* **1958,** *64*, 205-221.
33. Andersen, R. A., *Algal culturing techniques*. Elsevier, Academic Press [u.a.]: Amsterdam [u.a.], 2005.
34. Myers, D. K. *Harvesting Corn Residue*; Ohio State University Extension: Columbus, 2009.
35. PHYLLIS, Phyllis, database for biomass and waste,. In Energy research Centre of the Netherlands 2009.
36. Hirano, A.; Hon-Nami, K.; Kunito, S.; Hada, M.; Ogushi, Y., Temperature effect on continuous gasification of microalgal biomass: theoretical yield of methanol production and its energy balance. *Catalysis Today* **1998,** *45*, (1-4), 399-404.
37. Ross, A. B.; Jones, J. M.; Kubacki, M. L.; Bridgeman, T., Classification of macroalgae as fuel and its thermochemical behavior. *Bioresource Technology* **2008,** *99*, (14), 6494-6504.
38. Miles, T. R.; T. R. Miles, J.; Baxter, L.; Bryers, R. W.; Jenkins, B. M.; Oden, L. L. *Alkali deposits found in biomass power plants. A preliminary investigation of their extend and nature*; NREL: 1995; p 82.
39. Hughes, E.; Tillman, D. *FETC/EPRI BIOMASS COFIRING COOPERATIVE AGREEMENT*; Electric Power Research Institute (EPRI): 1997.
40. Sami, M.; Annamalai, K.; Wooldridge, M., Co-firing of coal and biomass fuel blends. *Progress in Energy and Combustion Science* **2001,** *27*, (2), 171-214.
41. Smeenk, J.; Brown, R. C.; Eckels, D. *Determination of vapor phase alkali content during biomass gasification*; 1999; pp p.961-967.
42. D'Jes˙s, P.; Boukis, N.; Kraushaar-Czarnetzki, B.; Dinjus, E., Gasification of corn and clover grass in supercritical water. *Fuel* **2006,** *85*, (7-8), 1032-1038.
43. Weidema, B. Ecoinvent Data v2.0. http://www.ecoinvent.org/
44. Evans, R. J.; Knight, R. A.; Onischak, M.; Babu, S. P. *Development of biomass gasification to produce substitute fuels*; Battelle Pacific NW Laboratory: Richland, WA, 1988.
45. BFIN, Bioenergy Feedstock Information Network. In NREL: 2009.
46. Demirbas, A., Potential applications of renewable energy sources, biomass combustion problems in boiler power systems and combustion related environmental issues. *Progress in Energy and Combustion Science* **2005,** *31*, (2), 171-192.
47. ETSU *Straw firing of industrial boilers*; ETSU: London, 1988.
48. Wilen, C.; Moilanen, A.; Kurkela, E. *Biomass feedstock analyses*; Thechnical research centre of Finland: 1996.
49. Schmidt, A.; Zschetzsche, A.; Hantsch-Linhart, W. *Analyse von biogenen Brennstoffen*; 1993.
50. Reisinger, K. nergetische Verwertungsmöglichkeiten von biogenen Reststoffen verschiedener Industriebranchen wowie aus kommunalen Sammelsystemen. TU Wien, Wien, 1997.

51. FEC *Straw Firing of Industrial Boilers*; Energy Technology Support Unit: Department of Energy, UK: 1988.
52. Zabaniotou, A.; Ioannidou, O.; Skoulou, V., Rapeseed residues utilization for energy and 2nd generation biofuels. *Fuel* **2008,** *87*, (8-9), 1492-1502.
53. IPCC, Changes in Atmospheric Constituents and in Radiative Forcing. In *Fourth Assessment Report (AR4) by Working Group 1 (WG1)* 2007.
54. Moulick, S.; Mal, B. C., Performance Evaluation of Double-Hub Paddle Wheel Aerator. *J. Envir. Engrg. Volume* **2009,** *135*, (7), 562-566.
55. Becker, E. W., *Microalgae: biotechnology and microbiology*. Cambridge University Press: Cambridge, 1994; p vii, 293 p.
56. Perry, R. H.; Green, D. W., *Perry's Chemical Engineers' Handbook*. 7th Edition ed.; McGraw-Hill: 2008.
57. Benemann, J. R.; Oswald, W. J. *Systems and economic analysis of microalgae ponds for conversion of CO(sub 2) to biomass. Second quarterly technical progress report, 16 December 1993--15 March 1994*; United States, 05, 1994; p 70.
58. Kurano, N.; Ikemoto, H.; Miyashita, H.; Hasegawa, T.; Hata, H.; Miyachi, S., Fixation and utilization of carbon dioxide by microalgal photosynthesis. *Energy Conversion and Management* **1995,** *36*, (6-9), 689-692.
59. Dodd, M. C.; Zuleeg, S.; Von Gunten, U.; Pronk, W., Ozonation of source-separated urine for resource recovery and waste minimization: Process modeling, reaction chemistry, and operational considerations. *Environmental Science and Technology* **2008,** *42*, (24), 9329-9337.
60. Kim, M. K.; Park, J. W.; Park, C. S.; Kim, S. J.; Jeune, K. H.; Chang, M. U.; Acreman, J., Enhanced production of Scenedesmus spp. (green microalgae) using a new medium containing fermented swine wastewater. *Bioresource Technology* **2007,** *98*, (11), 2220-2228.
61. Carey, R.; Migliaccio, K., Contribution of Wastewater Treatment Plant Effluents to Nutrient Dynamics in Aquatic Systems: A Review. *Environmental Management* **2009,** *44*, (2), 205-217.
62. Dodd, M.; Zuleeg, S.; Von Gunten, U.; Pronk, W., Ozonation of source-separated urine for resource recovery and waste minimization: Process modeling, reaction chemistry, and operational considerations. *Environmental Science and Technology* **2008,** *42*, 9329 – 9337.
63. VDEQ *Nutrients and the chesapeake bay*; Virginia Department of Environmental Quality: Richmond, 2007.
64. Maurer, M.; Schwegler, P.; Larsen, T. A., Nutrients in urine: Energetic aspects of removal and recovery. *Water Science and Technology* **2003,** *48*, (1), 37-46.
65. Purtschert, I.; Siegrist, H.; Gujer, W., Enhanced denitrification with methanol at WWTP Zürich-Werdhölzli. *Water Science and Technology* **1996,** *33*, (12), 117-126.